Martinez-Conde, Macknik, Martinez, Alonso & Tse (Eds.)
Progress in Brain Research, Vol. 155
ISSN 0079-6123

CHAPTER 17

Crossmodal audio–visual interactions in the primary visual cortex of the visually deprived cat: a physiological and anatomical study

M.V. Sanchez-Vives[1,*], L.G. Nowak[2], V.F. Descalzo[1], J.V. Garcia-Velasco[1], R. Gallego[1] and P. Berbel[1]

[1]*Instituto de Neurociencias de Alicante, Universidad Miguel Hernández–CSIC, Apartado 18, 03550 San Juan de Alicante, Spain*
[2]*Centre de recherche "Cerveau et Cognition". CNRS-Université Paul Sabatier 133, route de Narbonne, 31062 Toulouse Cedex, France*

Abstract: Blind individuals often demonstrate enhanced non-visual perceptual abilities. Neuroimaging and transcranial magnetic stimulation experiments have suggested that computations carried out in the occipital cortex may underlie these enhanced somatosensory or auditory performances. Thus, cortical areas that are dedicated to the analysis of the visual scene may, in the blind, acquire the capacity to participate in other sensory processing. However, the neural substrate that underlies this transfer of function is not fully characterized. Here we studied the synaptic and anatomical basis of this phenomenon in cats that were visually deprived by dark rearing, either early visually deprived after birth (EVD), or late visually deprived after the end of the critical period (LVD); data were compared with those obtained in normally reared cats (controls). The presence of synaptic and spike responses to auditory stimulation was examined by means of intracellular recordings in area 17 and the border between areas 17 and 18. While none of the cells recorded in control and LVD cats showed responses to sound, 14% of the cells recorded in EVD cats showed both subthreshold synaptic responses and suprathreshold spike responses to auditory stimuli. Synaptic responses were of small amplitude, but well time-locked to the stimuli and had an average latency of 30 ± 12 ms. In an attempt to identify the origin of the inputs carrying auditory information to the visual cortex, wheat germ agglutinin-horseradish peroxidase (WGA-HRP) was injected in the visual cortex and retrograde labeling examined in the cortex and thalamus. No significant retrograde labeling was found in auditory cortical areas. However, the proportion of neurons projecting from supragranular layers of the posteromedial and posterolateral parts of the lateral suprasylvian region to V1 was higher than that in control cats. Retrograde labeling in the lateral geniculate nucleus showed no difference in the total number of neurons between control and visually deprived cats, but there was a higher proportion of labeling in C-laminae in deprived cats. Labeled cells were not found in the medial geniculate nucleus, a thalamic relay for auditory information, in either control or visually deprived cats. Finally, immunohistochemistry of the visual cortex of deprived cats revealed a striking decrease in pavalbumin- and calretinin-positive neurons, the functional implications of which we discuss.

Keywords: plasticity; crossmodal; multisensory; visually deprived; critical period

*Corresponding author. Phone: (+34)965-919368;
E-mail: mavi.sanchez@umh.es

DOI: 10.1016/S0079-6123(06)55017-4

Introduction

Blind individuals often demonstrate enhanced non-visual perceptual abilities. Such enhanced perception has been widely documented for auditory spatial discrimination tasks (Ashmead et al., 1998; Lessard et al., 1998; Roder et al., 1999) as well as for tactile discrimination tasks (Merabet et al., 2004; Roder et al., 2004). Several lines of evidence support the suggestion that these improved performance could be due, at least in part, to the recruitment of the visual cortex for somatosensory or auditory processing following a process of cross-modal plasticity. First, there is an increased electrical activation of the visual cortex during pitch discrimination (Kujala et al., 1995) and during spatial discrimination for peripheral sound sources (Roder et al., 1999) in the early blind, which is not observed in sighted subjects. Second, functional imaging studies of people who were blind from an early age revealed that their primary visual cortex could be activated by Braille reading and other tactile discrimination tasks (Sadato et al., 1996). Third, the activation of the visual cortex appears to be functionally relevant, since the blockade of occipital processing by means of transcranial magnetic stimulation interferes with tactile performance in early blind but not in sighted individuals (Cohen et al., 1997; Gougoux et al., 2004; Merabet et al., 2004). An additional support for a role of the occipital cortex has recently been provided by a functional brain imaging study in which the activation of occipital cortex in early blind individuals was found to be positively correlated with performance in a monaural auditory localization task (Gougoux et al., 2005). Although some authors have found evidence of auditory-visual cross-modal plasticity in late-onset blindness (Kujala et al., 1997), it appears that the performance improvement in non-visual tasks is larger in subjects with early onset blindness (e.g. Gougoux et al., 2004). This observation is in agreement with the fact that the cerebral cortex is more prone to plasticity during the early years.

Human studies therefore show that visual cortex of blind people undergoes some modifications that allow its recruitment in the performance of non-visual tasks. Understanding how the visual cortex is taken over by other sensory modalities requires examining the neuronal basis of cross-modal plasticity, which can only be explored in animal models. Since the seminal studies of Wiesel and Hubel (1965), it is known that visual deprivation early in life had a large impact on the structure and the physiology of the visual system (Hubel et al., 1977; Sherman and Spear, 1982; Fregnac and Imbert, 1984). In addition to alterations in the visual system development and functioning, early visual deprivation also results in the appearance of response to non-visual modalities in areas that were exclusively or mainly visual in normal animals. For example, Hyvarinen et al. (1981) found somatosensory responses in 19% of the cells recorded in area 19 of monkeys deprived of sight by bilateral eyelid suture shortly after birth. The same study also mentions weak somatosensory responses in area 17. Toldi et al. (1988, 1994) also showed that, in rat monocularly enucleated at birth, somatosensory evoked responses invaded the visual cortex, including the anterior part of area 17. Rauschecker and Korte (1993) found that, in cats that had been visually deprived for several years, most of the cells located in the caudal part of the anterior ectosylvian cortex, which is normally dominated by the visual modality, had acquired auditory responses. Furthermore, these neurons showed better spatial tuning for sound source localization than those recorded in adjacent auditory territories in normal cats (Korte and Rauschecker, 1993). Recently, Yaka et al. (1999) found that the number of cells responding to auditory stimulation was larger in two extrastriate areas (areas ALLS and AMLS) in cats that were visually deprived shortly after birth, either by eyelid suturing or by enucleation. Auditory responses were also obtained in 6% of the cells recorded in area 17 of the enucleated cats, but not in normal and eyelid-sutured cats (Yaka et al., 1999, 2000). Crossmodal plasticity also has been documented in the visual cortex of neonatally enucleated hamsters (Izraeli et al., 2002), where 63% of the cells were found to respond to auditory stimuli.

In this study we examined, at the physiological and anatomical levels, how the auditory modality becomes able to generate neuronal activity in the visual cortex of visually deprived cats. Cats were deprived of vision by rearing them in the dark for

several months to 1 year. Deprivation started either immediately after birth (early visually deprived cats, EVD group) or at a mature age (late visually deprived cats, LVD group). The physiological study consisted in recording intracellularly from neurons in area 17 and in the 17/18 border region (Fig. 1). Our aim was to detect synaptic, subthreshold responses to sound stimulation, which could have remained undetected if recorded extracellularly. To identify possible new inputs to the visual cortex of deprived cats, retrograde tracers were injected in the equivalent areas in the hemisphere contralateral to the one from which recordings were obtained. The number of retrogradely labeled neurons were quantified in various cortical and thalamic areas. Finally, immunohistochemical staining of inhibitory neurons allowed us to examine the consequences of visual deprivation on inhibition in cortex, changes that explain a number of functional observations that are found in visually deprived animals.

Methods

Thirteen cats of either sex were included in this study, including physiological and diverse anatomical studies (see below). Five of these cats were born and reared in a normal environment (control cats) and eight were visually deprived. Among these eight visually deprived cats, three were deprived as adults (aged 4 months to 3 years) by placing them in a dark room for 3–7 months until the day of the experiment. We will refer to them as the LVD group, since deprivation took place after the end of the critical period. The remaining five cats were born and raised in a dark environment until the time of recording (aged 6 months to 1 year) and they correspond to the EVD group.

All but one of the anatomical studies (immunohistochemistry and retrograde labeling) were carried out in the animals in which the electrophysiological studies were done.

Visual deprivation

Control cats were reared in a 12 h light/dark cycle. Visually deprived cats were kept in a pitch-black dark room. We chose this method rather than enucleation for its reversibility, and rather than lid-suture, since that method does not guarantee total absence of visual stimulation (Spear et al., 1978). Animal caretakers walked into the cats' room from a darkened hallway, and were provided with a helmet carrying a video camera with infrared lighting (GL 380, SHARP®; λ peak = 950 nm) that allowed them to maintain the room clean, check the state of the animals and replace food and water. Another video camera sensitive to infrared, located inside the animal room, allowed us to check the animals' state and behavior on a monitor from outside the room. In order to create a sound-rich environment, four different sounds (pure tones between 2 and 20 kHz; 65 dB) coming from four speakers in the different walls of the room were used for alternate stimulation for 2–6 h/day.

The project was approved by the local ethical committee. Local rules comply with the EU guidelines on protection of vertebrates used for experimentation (Strasbourg 3/18/1986, Spanish law BOE 256; 10/25/1990).

Animal preparation for in vivo recording

Intracellular recordings "*in vivo*" from the visual cortex of cats were obtained following the methodology that we have previously described (Sanchez-Vives et al., 2000b), except for the anesthetic used during the recordings. In short, adult cats were anesthetized with ketamine (12–15 mg/kg, i.m.) and xylazine (1 mg/kg, i.m.) and then mounted in a stereotaxic frame. A craniotomy (3–4 mm wide) was made overlying the representation of area 17. To minimize pulsation arising from the heartbeat and respiration, a cisternal drainage and a bilateral pneumothorax were performed, and the animal was suspended by the rib cage to the stereotaxic frame. During recording, anesthesia was maintained with continuous i.v. infusion of propofol (5 mg/kg/h) and sufentanyl (4 μg/kg/h) and the animal was paralyzed with norcuron (induction 0.3 mg/kg; maintenance 60 μg/kg/h) and artificially ventilated. The heart rate, expiratory CO_2 concentration, rectal temperature and blood O_2 concentration were monitored throughout the experiment and maintained at 140–180 bpm, 3–4%, 37–38 °C and > 95%, respectively. The electroencephalogram (EEG) and

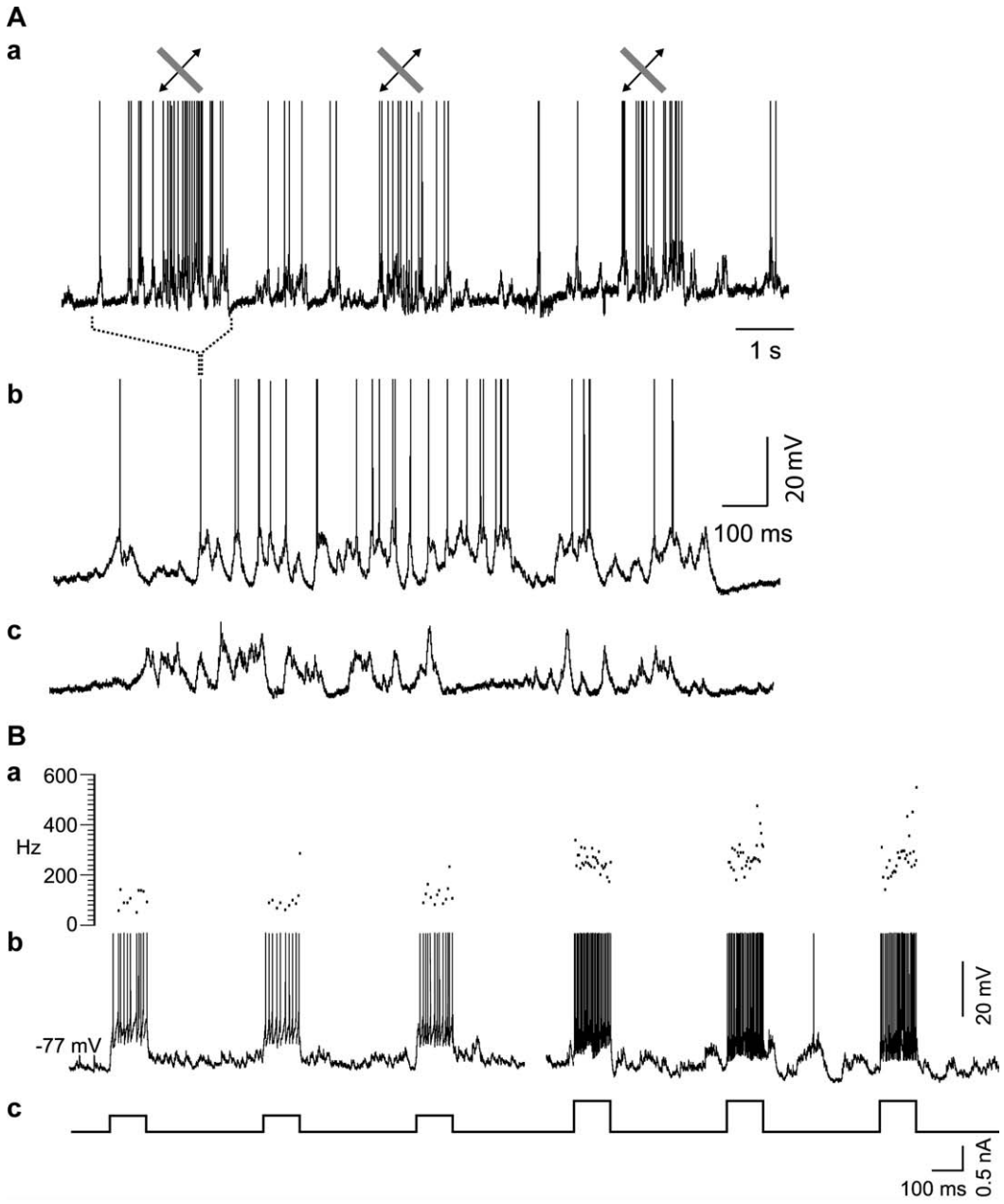

Fig. 1. Electrophysiological recordings from the visual cortex of control and visually deprived cats. (A) Visual responses recorded in control cats and evoked by moving bars with a handheld projector onto the tangent screen. (Aa) Synaptic and spike responses to three consecutive visual stimuli. (Ab) First visual response expanded. (Ac) Subthreshold (synaptic) visual response. (B) In visually deprived cats, no visual stimuli were used (see the section "Results") but responses to pulses of injected currents were recorded. This panel shows responses to current injections in a neuron that was characterized as fast-spiking neuron (according to Nowak et al., 2003) and showed both sub- and suprathreshold reponses to sound (not shown). From top to bottom: instantaneous frequency, membrane voltage and current are shown. Notice the spontaneous synaptic activity in between pulses and how synaptic activity affected the frequency of discharge as reflected in the variability in the instantaneous frequency. Spikes have been truncated.

the absence of reaction to noxious stimuli were regularly checked to insure an adequate depth of anesthesia. After the recording session, the animal was given a lethal injection of sodium pentobarbital.

Recordings and stimulation

Sharp intracellular recording electrodes were made with a Sutter Instruments (Novato, CA) P-97 micropipette puller from medium-walled glass capillaries and beveled to final resistances of 50–100 MΩ. Micropipettes were filled with 2 M KAc. Recordings were digitized, acquired and analyzed using a data acquisition interface and software from Cambridge Electronic Design (Cambridge, UK). In control animals, the eyes were focused onto a tangent screen at 114 cm using corrective, gas-permeable contact lenses. The position of the area centralis and optic discs was localized by retroprojection. Receptive field's location was determined with a handheld projector. In dark-reared animals the eyes were covered during the experiments.

Auditory stimulation

Pure tones at various frequencies (1–20 kHz), white noise and clicks were used as auditory stimuli. Pure tones were generated using a waveform generator (Racal Dana 9085 Low Distorsion Oscillator). White noise was generated with a noncommercial generator. The signals were trapezoidally gated with rise/fall times of 5 ms. Stimuli onset and duration were controlled by a computer. The stereotaxic frame had hollow ear bars and the loudspeakers were placed inside. Thus, stimuli were delivered binaurally through a closed acoustic system based on Sony MDR E-868 earphones housed in a metal enclosure and surrounded by damping material which fitted into the Perspex specula (Rees et al., 1997). The output of the system for each stimulus was calibrated to be between 60 and 80 dB.

Analysis

Each run of auditory stimuli lasted for 150–700 s. For each run, the membrane potential was averaged with respect to the auditory stimulus trigger (black trace in Fig. 2Ab). The mean potential between 15 and 165 ms (or 115 ms in case shorter stimulus duration was used) was calculated. The mean potential between –150 (or –100) and 0 ms was calculated as well to give a mean baseline value. The mean baseline value was subtracted to give the mean membrane potential depolarization above baseline, or mean stimulus-locked response amplitude (MRA_{SL}, black bin in Fig. 2Ac). The spike response (Fig. 2B) was calculated as a peristimulus time histogram (PSTH) with a bin width of 10 ms. The measured variable in this case was the average firing rate above spontaneous activity in a time window between 15 and 165 (or 115) ms relative to auditory stimulus onset, yielding the MRA_{SL} (dark bin in Fig. 2Bc). The significance of the response was evaluated using a Monte Carlo simulation. The hypothesis underlying the use of the Monte Carlo method is as follows: on the one hand, the synaptic potential observed in the membrane potential average (or firing rate changes in the PSTH) may result from the preceding auditory stimulus, in which case they should be stimulus locked. On the other hand, the membrane potential in anesthetized preparations often shows spontaneous synaptic activity characterized by large fluctuations (Fig. 1Aa), reaching up to 20 mV amplitude, due to a slow wave sleep rhythm (Steriade et al., 1993; Sanchez-Vives and McCormick, 2000). If the deviations obtained in the membrane potential average were due to spontaneous synaptic activity, then the amplitude should be independent of the precise stimulus trigger timing.

To confront these two possibilities, each "real" auditory trigger occurring at time t was replaced by a randomly jittering trigger (Figs. 2Aa and 2Ba). The new trigger had a time of occurrence limited to $t+\alpha$, α being an added delay that took a random value within a range between $-0.5\,T$ and $+0.5\,T$, T being the period of the "real" auditory trigger. This procedure was repeated for all the triggers, with a new α value for each trigger. The membrane potential average or the PSTH was recalculated and the amplitude of the response measured as above. Figure 2Ab represents five traces of membrane potential averages triggered by random triggers in addition to the one obtained with the regular

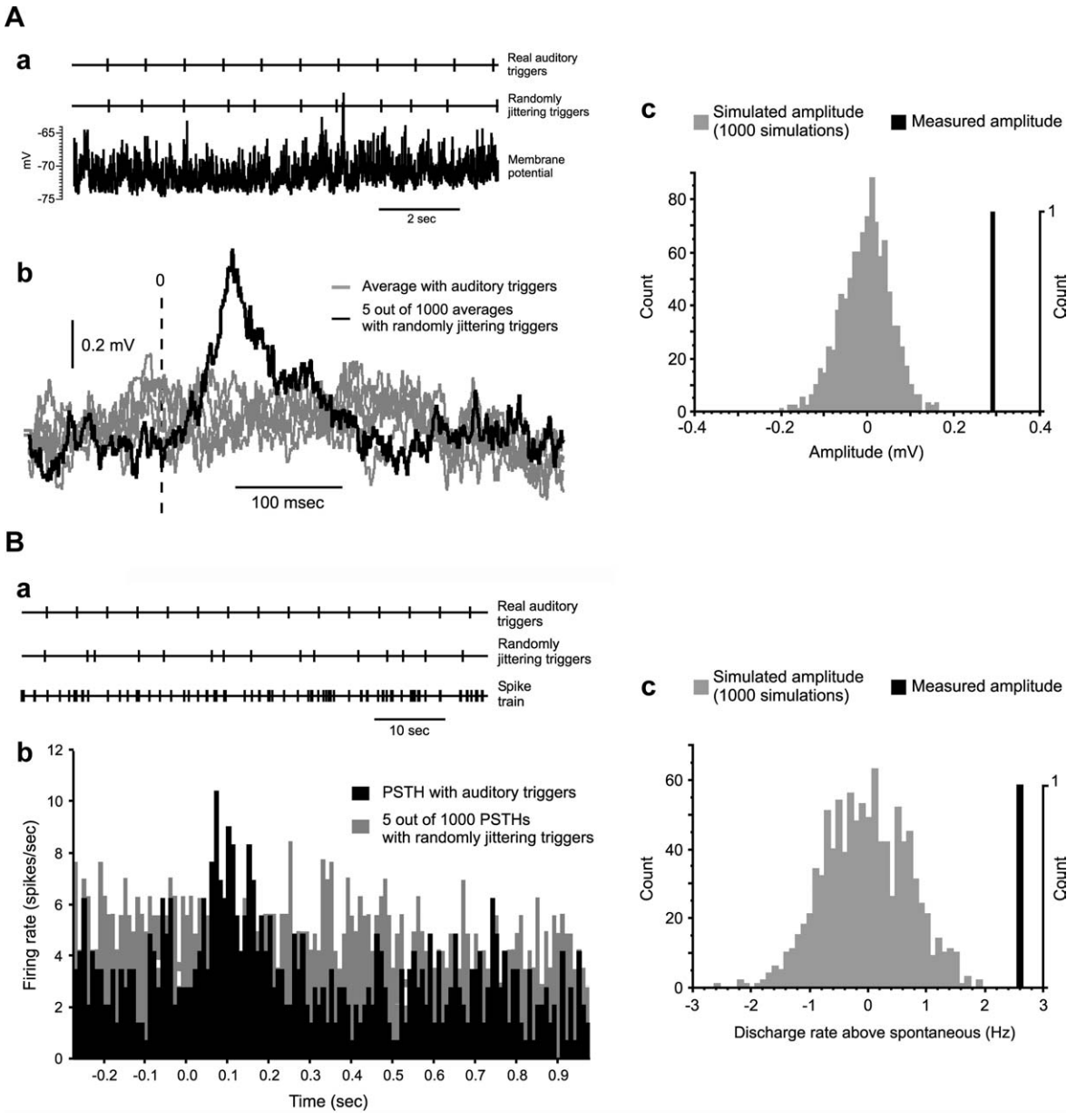

Fig. 2. Detection of significant synaptic and spike responses with a Monte Carlo method. (A) Detection of significant synaptic responses by using a Monte Carlo simulation (Aa) From top to bottom: example of auditory triggers, randomly generated triggers (see the section ''Methods'') and voltage trace corresponding to the intracellular recording. (Ab) Five traces (in gray) corresponding to the membrane voltage average triggered with five randomly selected triggers and one trace (in black) corresponding to the voltage average triggered with the real auditory triggers. (Ac) Distribution of amplitudes for 1000 voltage averages triggered with random series of triggers (in gray). In black, on the right, the amplitude of the voltage average triggered with the real auditory triggers. The amplitude corresponds to the mean amplitude between 15 and 165 ms relative to auditory stimulus onset in the averages, minus baseline. (B) Detection of significant spiking responses by using a Monte Carlo simulation (Ba) From top to bottom: example of auditory triggers, randomly generated triggers (see the section ''Methods'') and events corresponding to intracellularly recorded action potentials. (Bb) PSTHs obtained with the auditory trigger appears in black and five PSTHs obtained with randomly jittering triggers in gray. (Bc) Distribution of amplitudes for 1000 PSTHs triggered with random series of triggers (in gray). In black, on the right, the amplitude of the PSTH triggered with the real auditory triggers. The amplitude corresponds to the firing rate between 15 and 165 ms relative to auditory stimulus onset in the PSTHs, minus spontaneous activity.

auditory trigger. The same procedure was applied to the spike responses (Fig. 2Bb).

The simulation was repeated 1000 times. The distribution of mean depolarization calculated for 1000 averages is shown by the gray bars in the histogram in Fig. 2Ac. The distribution of these values corresponds to the distribution of amplitudes one would get if the depolarization was not locked to the stimulus, i.e., noise consecutive to spontaneous activity. This distribution shows the typical shape of a normal distribution, which can be characterized by a mean μ and a standard deviation σ. The MRA_{SL} was standardized as a z value as $z = (MRA_{SL} - \mu)/\sigma$. Since z will have a standard normal distribution ($\mu = 0$; $\sigma = 1$), it can be easily used to calculate the probability that the sound-evoked response is spurious resulting from spontaneous activity instead of an event-locked auditory response. Membrane potential average and average spike responses were considered as significant auditory responses when z values were outside the ± 1.96 range ($p = 0.05$; Fig. 2Ac for synaptic responses and Fig. 2Bc for spike responses; z value of ± 2.58 corresponds to a p value $= 0.01$). This method provided a reliable and sensitive indicator of the presence of auditory responses in cat visual cortex. Whenever a significant response was obtained, the latency and amplitude were determined. The latency corresponds to the first of two consecutive bins that showed an amplitude larger than the mean baseline + 3 SD. Amplitude is the peak amplitude *minus* mean baseline.

Retrograde labeling

A total of four control, four EVD and one LVD cats were included in the tracer injection's study. Under anesthesia (see preparation for *in vivo* recordings above), each cat received 3–5 injections (0.1 µl each) of 10% HRP coupled to WGA-HRP in physiological saline. Injections were made near the 17/18 border expanding to areas 17, 18 and 19, at a depth of 900 µm and were evenly spaced from one another (23–19 mm caudally from *bregma* and 1.5–2 mm lateral). Tracer was delivered by pressure pulses (Picopump, WPI) through glass pipettes (outer diameter of the tip 40–60 µm). After 1–2 days survival, the anesthetized cats were perfused with physiological saline for 5 min followed by 1% paraformaldehyde, 0.5% glutaraldehyde, 0.002 M $CaCl_2$ and 0.1 M saccharose in 0.1 M phosphate buffer (pH 7.3–7.4) for 30 min. The brains were removed and cryoprotected, and 60 µm-thick slices were cut in the coronal plane using a cryostat into two parallel series. One series was mounted on gelatinized slides and air-dried for 24 h and stained in 1% cresyl violet (Sigma, St. Louis, MO, USA). The other series were floating sections that were processed with 3,3′,5,5′-tetramethylbenzidine (Mesulam, 1978). Reacted sections were mounted on gelatinized slides, air-dried for 24 h, briefly dehydrated and cleared in xylene, and mounted in Eukitt (O. Kindler GmbH & Co, Freiburg, Germany). Injections covered a large extent of the visual areas 17 and 18.

Histo- and immunochemistry

Four control, four EVD and one LVD cats were processed for immunohistochemistry. They were perfused with physiological saline for 5 min followed by 4% paraformaldehyde, 0.002 M $CaCl_2$, and 0.1 M saccharose in 0.1 M phosphate buffer (pH 7.3–7.4) for 30 min.Brains were cut using a vibratome in slices 100 µm-thick into four parallel series. One series was mounted on gelatinized slides and air-dried for 24 h and processed for CO staining, being incubated in freshly prepared 0.06% DAB, 0.02% cytochrome C, type III (Sigma) and 4.25% sucrose in PBS for 16–24 h at 37 °C (Wong-Riley, 1979). Three series were immunostained with markers (calretinin, calbindin and parvalbumin) revealing different subtypes of GABAergic neurons (Celio, 1990; Celio et al., 1990; DeFelipe, 1997). Floating sections were incubated with rabbit anti-calretinin Ab (1:2000; Swant, Bellinzona, Switzerland), which was followed with biotinylated goat anti-rabbit Ab (1:150; Vector), ABC kit and DAB. The other two series were stained with anti-parvalbumin (1:1000; Swant) and anti-calbindin D-28 K (1:2000; Swant) monoclonal antibodies. Immunostaining was followed by biotinylated horse anti-mouse Ab (Vector), ABC kit and DAB. Immunostained sections were mounted on gelatinized slides, air-dried for 24 h, dehydrated in ethanol, cleared in xylol and coverslipped.

Quantitative anatomical analysis

Sections were studied and photographed using an Olympus BX50W1 microscope with a Nikon D70 digital camera. Plots and counts of immunoreactive and retrogradely labeled cells were obtained using the Neurograph system (Microptic, Barcelona, Spain). Retrogradely labeled neurons in the following areas were plotted: ipsilaterally, the posteromedial lateral suprasylvian visual area (PMLS) and the posterolateral lateral suprasylvian visual area (PLLS), auditory areas I and II (AI and AII), the medial geniculate nucleus (MGN), the dorsal lateral geniculate nucleus (dLGN) and the medial interlaminar nucleus of the dLGN (MIN); contralaterally, visual areas 17, 18, PMLS and PLLS, and the auditory area AI. The entire cross-sectional coronal surface of the MGN, dLGN and MIN was analyzed. In all cases, the borders between cortical layers and dLGN laminae were placed at the same relative depth, measured from adjacent sections stained with cresyl violet. In addition, cells immunoreactive to parvalbumin, calbindin D-28 K and calretinin in areas 17 and 18 were also plotted. For quantitative analysis of both immunohistochemistry and retrograde labeling, cells were counted within a rectangular area (probe) that measured 200 μm wide and spanned from layer I to the subcortical white matter. In studies of retrograde labeling these probes covered the entire studied cortical areas. In immunohistochemical studies three probes evenly spaced in areas 17 and 18 were quantified. In total, three sections per area and animal were quantified and the mean number was then averaged among animals within each experimental group. The Systat statistical software (Systat Inc., Evanston, IL) was used for one-way ANOVAs, followed by Tukey's test to identify significant differences ($p \leqslant 0.05$) between means.

Results

Functional study of auditory responses in the visual cortex

Ten cats were included in the electrophysiological study. Three of these cats were born and reared in a normal environment (control cats) and seven were visually deprived. Out of these seven visually deprived cats, four were visually deprived as adults (aged 4 months–3 years) by placing them in a dark room for 3–7 months until the day of the experiment. We will refer to them as the LVD group, since deprivation took place after the end of the critical period. The remaining three cats were born and raised in a dark environment until the time of recording (aged 6 months–1 year) and they correspond to the EVD group.

Intracellular recordings that were sufficiently long and stable to allow the characterization of auditory responses in visual cortex were obtained from a total of 148 cells. Of these, 32 were recorded in control cats, 60 in LVD cats and 56 in EVD cats. For a representative sample of 20 neurons in control and 20 in visually deprived cats the input resistance was 26.7 ± 10.07 and 27.5 ± 14.8 MΩ, respectively, and the membrane time constant was 32.0 ± 8.9 and 26.7 ± 9.3 ms, respectively.

The objective of these experiments was to examine the possible existence of auditory responses in the visual cortex of the three experimental groups. Intracellular recordings were performed to be able to detect subthreshold synaptic responses that could have been overlooked if the recordings would have been extracellular. For this reason, and in order to better detect synaptic responses, during some of the recordings the membrane potential was hyperpolarized to prevent spiking activity and therefore only subthreshold synaptic responses were analyzed. In the other cells, both spiking and synaptic responses were recorded and analyzed.

Once an intracellular recording was obtained and the intrinsic membrane properties were measured, sensory stimulation began. In both experimental groups, control and visually deprived cats, the level of anesthesia was as in our previous studies of visual responses (Sanchez-Vives et al., 2000a; Nowak et al., 2003) and therefore compatible with the existence of sensory responses. This was directly checked in control cats, where visual responses to bars of light were explored with a handheld projector to ensure that neurons were visually responsive (Fig. 1A). No further characterization of visual responses was done, in order to concentrate on the auditory stimulation. In EVD and LVD cats no visual stimuli were delivered, to prevent reversion or decline of any auditory

responses that could have developed during the period of visual deprivation. Auditory stimulation was delivered through headphones placed inside the ear bars and consisted of white noise, pure tones (1–20 kHz) and/or clicks. Stimulus duration was 150–2000 ms for tones and white noise, and 10–20 ms for clicks, and the stimuli were given at a frequency of 0.5–2 Hz.The responses to auditory stimuli were evaluated for both membrane potential values and spike response (PSTH), by calculating the spike-triggered average with respect to the auditory stimulus. The significance of this response was estimated by using a Monte Carlo simulation. In short, 1000 random triggers (Figs. 2Aa, Ba) were generated and used for spike-triggered average of both the membrane potential (Fig. 2Ab) and the spike response (Fig. 2Bb), and compared with the actual auditory-locked responses (for details see ''Methods'').

The distribution of the standardized responses to both auditory and random triggers (z values; $\mu = 0$; $\sigma = 1$; see ''Methods'') for the synaptic and spiking response and for the three experimental groups of cats is shown in Fig. 3. None of the 32 cells recorded in control cats showed any significant response to auditory stimuli ($-1.96 < z < 1.96$, Figs. 3Aa, Ba). Similarly, none of the 60 cells recorded in the LVD cats showed any significant response to sound stimuli (Figs. 3Ab, Bb). However, significant responses have been observed in the EVD cats, both for synaptic and spiking responses (Figs. 3Ac, Bc). The total number of cells showing significant responses to sound stimuli was 8 out 56 cells tested. This represents 14% of the cells recorded in the EVD animals. In three out of these eight neurons, only the synaptic response was recorded because the neurons were maintained subthreshold during the study. In three additional neurons both spiking and synaptic auditory responses were significant, and in the remaining two neurons, only the spiking response was significant — in these later cases, the spontaneous activity level was high and the continuous firing resulted in a strong shunt of the membrane potential that masked the synaptic response.

Hence in this study we describe, to our knowledge for the first time, synaptic potentials induced by sound in primary visual cortex. Fig. 4 shows both sub- and suprathreshold auditory responses from the same neuron. Although the average synaptic response (Fig. 4A) had an amplitude of only 0.5 mV, it was statistically significant and able to generate a significant suprathreshold response. This averaged spike response is represented in a PSTH in Fig. 4B and is overlapped with the synaptic response to illustrate their parallel time courses.

The amplitude of the averaged synaptic responses varied between 0.1 and 1.8 mV and the actual values for each of the six neurons in which synaptic responses were obtained in response to one or several auditory stimuli are shown in Fig. 5B. At the population level the mean amplitude was 0.6 ± 0.6 mV (only one value per neuron was used by prior averaging of the amplitude for the different auditory stimuli, when more than one was obtained in the same cell). The mean onset latency of the synaptic responses was 30 ± 12 ms (range 15–46 ms).

The average peak-firing rate obtained in response to auditory stimulation was 3.2 ± 2.4 spikes/s, and the mean onset latency of the spike response was 42 ± 24 ms. In three cases, the response to different kind of auditory stimuli was examined in the same cell. The synaptic responses (auditory-triggered average membrane potential) to different pure tone frequencies and to white noise stimulation are depicted for one of these cells in Fig. 5A. The graph shows that this cell was poorly tuned for specific frequencies and that the neuron responded with a depolarization to all the given auditory stimuli. This also was the case with the remaining two neurons (Fig. 5B).

Cytoarchitecture of the visual cortex in visually deprived cats

In order to better understand the structural basis underlying the functional phenomena that we have described in the previous section, we performed a number of anatomical studies in the same experimental groups in which the physiology was studied.

The cytoarchitecture of cortical areas 17 and 18, studied in cresyl violet-stained sections, was similar between control, EVD and LVD cats. Cortical

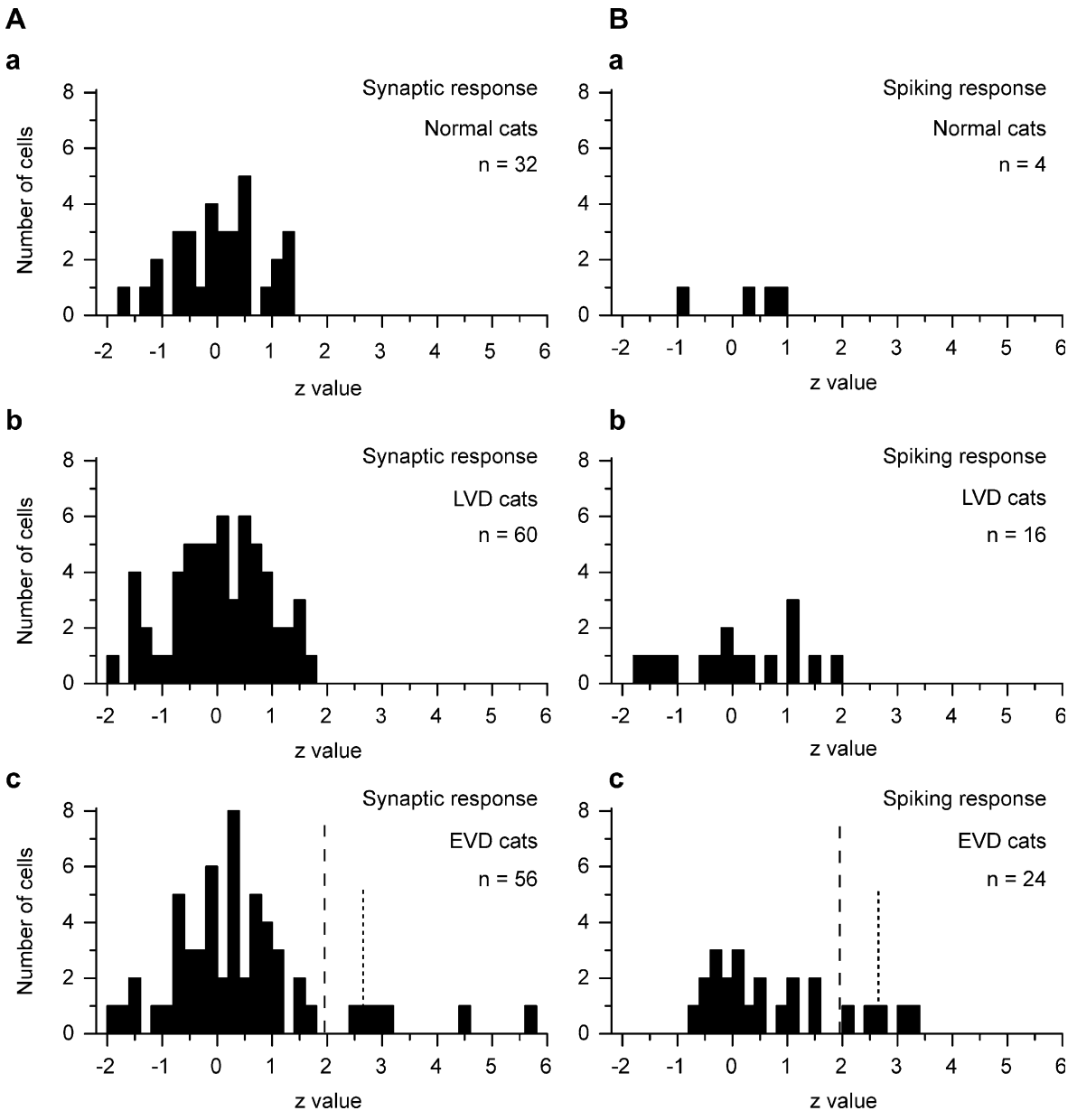

Fig. 3. Distribution of z-values for the PSPs recorded in control, EVD and LVD cats. (A) Distribution of z-values for synaptic responses. (Aa) Control cats. (Ab) LVD cats. (Ac) EVD cats. Notice that five of the z-values were above 1.96 and therefore significant at $p<0.05$. (B) Distribution of z-values for spike responses. (Ba) Control cats. (Bb) LVD cats. (Bc) EVD cats. Notice that five of the z-values were above 1.96 and therefore significant at $p<0.05$.

layers were present and the borders between layers well defined.

CO staining was made to identify layer IV in the cortical areas of control and EVD cats (no LVD cats were studied here). No differences were found between control and EVD cats in the differential intensity of the staining among cortical layers. In both experimental groups, layer IV was more

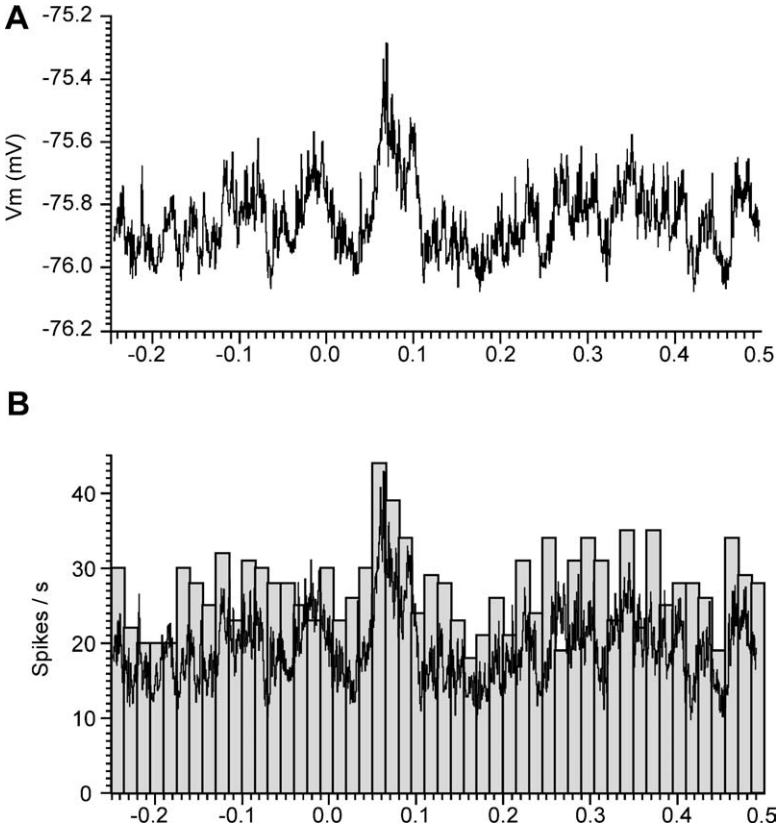

Fig. 4. Synaptic responses to sound in primary visual cortex. (A) Sound-triggered average of the membrane potential for a significant synaptic response. (B) PSTH of the suprathreshold, spiking response in the same neuron. Notice the similar time course to that for the synaptic response (shown in overlap).

intensely stained than the other layers, showing scattered, CO-stained pyramidal neurons in layer V (Fig. 6). However, the heavily stained band of layer IV had borders with adjacent layers III and V that were more blurred in EVD than in control cats (Fig. 6).

Distribution of intracortical retrogradely labeled neurons

Four control, four EVD and one LVD cats were injected with retrograde tracers in area 17, border of area 17/18 and areas 18 and 19 (see the section ''Methods''). No differences either in the distribution or in the density of labeled neurons were found between control and LVD cats; the LVD case is therefore not described further.

Ipsilateral projections from PMLS to areas 17 and 18

In all cases tracer core injection was near the 17/18 border; however, the tracer diffused to areas 17, 18 and 19, filling the postlateral girus (see inset in Fig. 7). The mean number of ipsilaterally projecting neurons per section from PMLS to areas 17 and 18 in EVD cats (872 ± 104 neurons per section) was not significantly different from the one in control cats (766 ± 194 neurons per section). However, the radial and tangential distribution of labeled neurons was qualitatively different (Figs. 7 and 8A). In control cats, the radial distribution of labeled neurons found in PMLS was similar to that previously described (Bullier et al., 1984b; Symonds and Rosenquist, 1984; Segraves and Innocenti, 1985; Kato et al., 1991; Shipp and

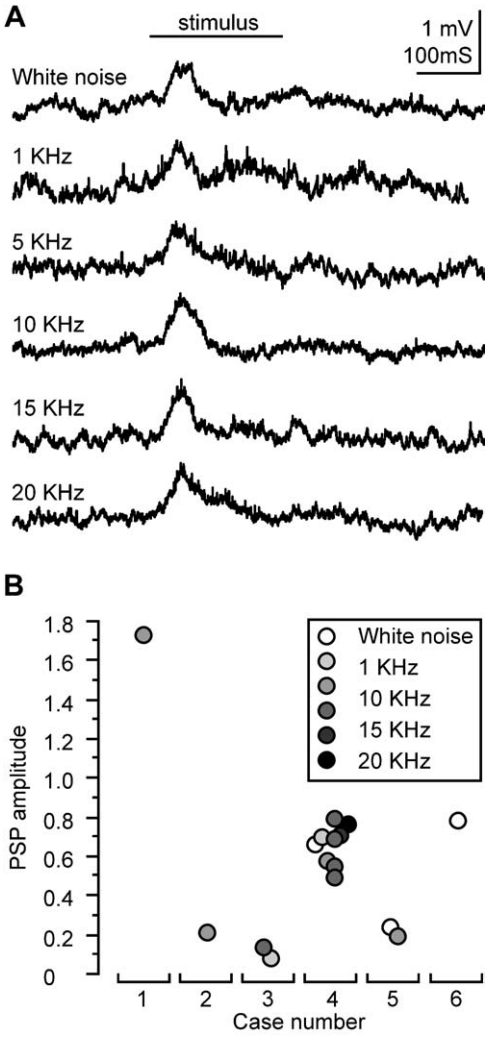

Fig. 5. Responses to white noise and pure tones at different frequencies in the visual cortex of the cat. (A) Synaptic responses to different auditory stimuli (white noise and pure tones at 1, 5, 10, 15 and 20 kHz). Each one is the result of averaging 526, 261, 332, 423, 398 and 423 stimuli, respectively. (B) Amplitudes of synaptic responses that were statistically significant ($p<0.05$) for each one of the six neurons and for the different sound stimuli.

Grant, 1991; Einstein, 1996; Batardière et al., 1998; Payne and Lomber, 2003). Thus, ipsilaterally projecting neurons from PMLS to areas 17 and 18 were mostly found in infragranular layers (layer V: 19.6%, and layer VI: 59.0%) and were less numerous in supragranular layers (layers II–III: 16.7% from the total). A small percentage of labeled neurons was also seen in layer IV (4.7%; Figs. 7A–C and 8A). In EVD cats, the proportion of retrogradely labeled neurons in layers IV (5.2%), V (15.0%) and VI (49.7%) was similar to controls, while it significantly increased in supragranular layers II–III (30.0%; Figs. 7D–F and 8A).

Contralateral projections from PMLS to areas 17 and 18

In control cats, the pattern of labeling in area PMLS contralateral to the injection site appears similar to that previously described (Keller and Innocenti, 1981; Segraves and Rosenquist, 1982; Segraves and Innocenti, 1985). Contralaterally projecting neurons from PMLS to areas 17 and 18 were mostly found in layers V (66.7%) and VI (33.3%). In EVD cats, the mean number of contralaterally projecting neurons per section from PMLS to areas 17 and 18 (109.8 ± 12.4 neurons per section) was significantly higher than in control cats (17.1 ± 7.1 neurons per section). The radial and tangential distribution of labeled neurons was also quantitatively different (Fig. 8A). In EVD cats, a large fraction of labeled neurons was found in layers II–III (34.4%), suggesting stabilization of connections that are transitory during development (Innocenti and Clarke, 1984). Neurons were also found in layer IV (18.7%). Given these relative increases in supragranular and layer IV labeling, the relative proportion of labeled neurons in layers V (26.8%) and VI (20.1%) was significantly decreased (Fig. 8A).

Ipsilateral projections from PLLS to areas 17 and 18

Ipsilaterally, the mean number of projecting neurons per section from PLLS to areas 17 and 18 in EVD cats was reduced with respect to controls (on average, 584 ± 112.6 neurons per section in control vs. 248 ± 92.4 neurons in EVD cats) and its radial distribution was also qualitatively different (Figs. 7 and 8A, B). In control cats, the radial distribution of labeled neurons found in PLLS was similar to that previously described (Symonds and Rosenquist, 1984; Rosenquist, 1985; Segraves and Innocenti, 1985; Payne and Lomber, 2003) (Fig. 7A). Ipsilaterally projecting neurons from

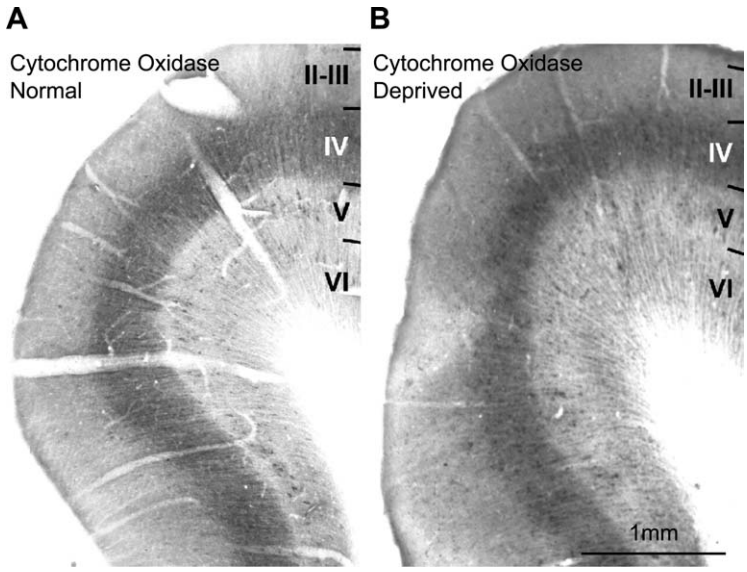

Fig. 6. Photomicrographs showing cytochrome oxidase labeling in coronal sections through area 17 of control (A) and EVD (B) cats. In layer IV of normal and EVD cats, dense CO staining can be seen. In deprived cats, CO labeling shows blurred borders between layer IV and layers II–III and V. Borders between layers are indicated. Same magnification for A and B.

PLLS to areas 17 and 18 were mostly found in infragranular layers (layer V: 18.3%; layer VI: 76.9%), also in layers II–III (3.3% from the total) and in layer IV (1.5%) (Figs. 7A–C and 8B). In EVD cats, the proportion of labeled neurons in layers II–III (13.1%) increased with respect to controls, whereas it was similar in layers IV (2.0%), V (12.1%) and VI (72.8%; Figs. 7D–F and 8B). In control and deprived cats, labeled neurons were mostly found in the medial half of the PLLS, close to the PMLS border located deep in the medial suprasylvian sulcus (Figs. 7D–F).

Contralateral projections from PLLS to areas 17 and 18

Contralaterally, the mean number of projecting neurons per section from PLLS to areas 17 and 18 in control cats was very low (on average, 2.8 ± 0.7 neurons per section). Although this number was also low in EVD cats (8.1 ± 1.4 neurons per section), it was significantly higher than in control cats. Both in control and EVD cats, contralaterally projecting neurons from PLLS to areas 17 and 18 were mostly found in layer VI, as shown previously (Keller and Innocenti, 1981). No labeled neurons were observed in other suprasylvian areas such as the AMLS and ALLS.

Projections from AI and AII to areas 17 and 18

No differences were found between control and both groups of deprived cats in the mean number of neurons per section and distribution of labeled neurons found in AI and AII. In all experimental groups, there were few neurons labeled per section (between 3 and 15), located near the fundus and anterior bank of the posterior ectosylvian sulcus as well as on the convexity of the middle ectosylvian and sylvian gyri, corresponding to areas AI and AII. Almost all labeled cells were located in the infragranular cortical layers. The distribution and numbers of labeled neurons were very similar to those already described for normal cats (Dehay et al., 1984; Innocenti and Clarke, 1984; Innocenti et al., 1988; Payne and Lomber, 2003).

Distribution of thalamic retrogradely labeled neurons

In both control and visually deprived cats, labeled neurons were found in all laminae of the dLGN, as described previously (Maciewicz, 1975; Hollander and Vanegas, 1977; Bullier et al., 1984a; Payne and

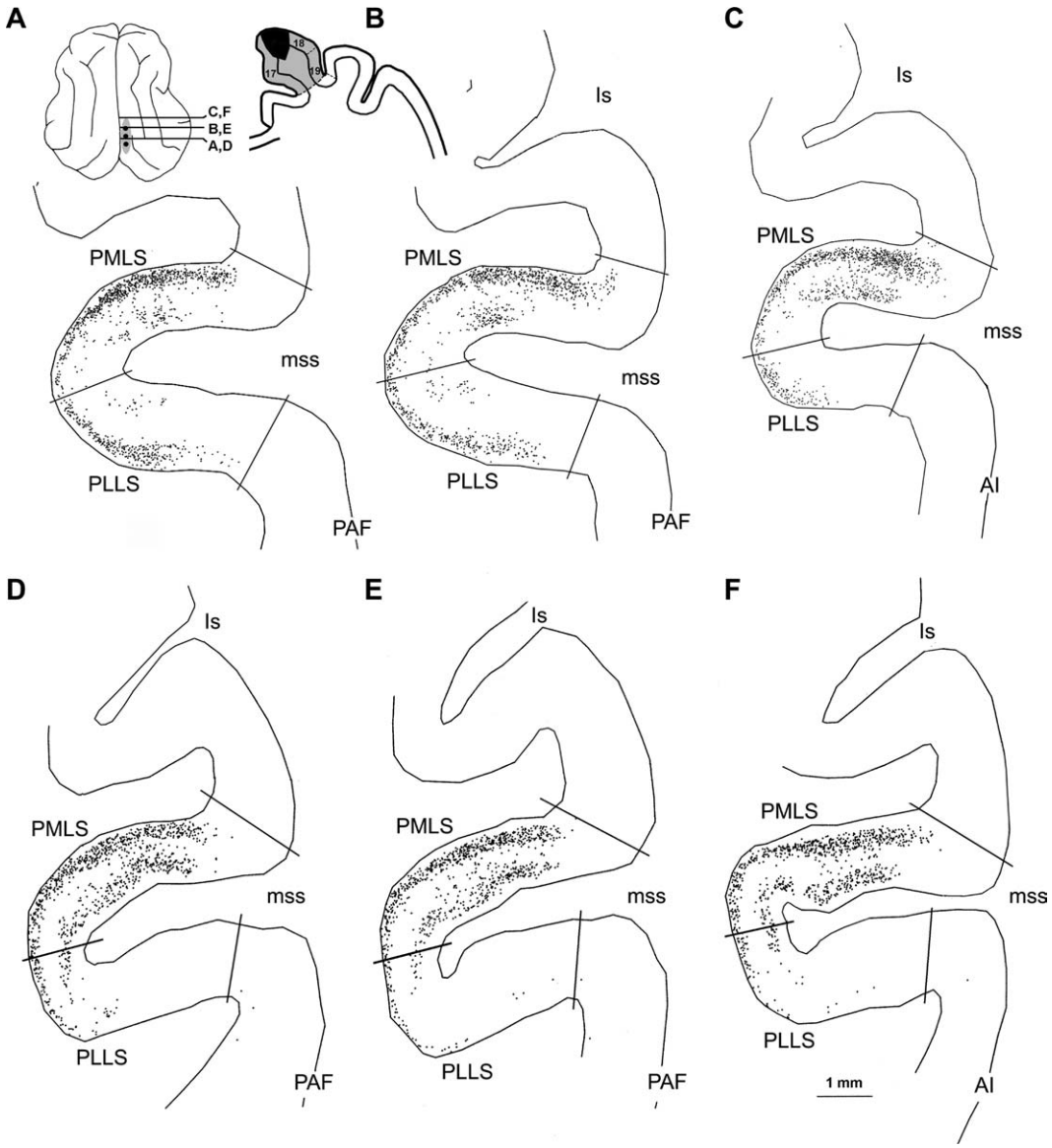

Fig. 7. Distribution of retrogradely labeled neurons in ipsilateral PMLS and PLLS following WGA-HRP injections in areas 17 and 18 in control (A–C) and EVD (D–F) cats. In control cats, labeling was found principally in infragranular layers. In EVD cats, the proportion of labeled neurons in supragranular layers increased with respect to controls. Note the reduced number of labeled neurons in the PLLS in EVD compared to control cats. Levels of sections, place (small black circles) and extent of injections (shaded areas) are shown in the brain figurines at the upper left corner. ls: lateral sulcus; mss: medial suprasylvian sulcus; PAF: posterior auditory field of the ectosylvian gyrus.

Lomber, 2003). However, in EVD cats they were more uniformly distributed in the mediolateral dimension. The proportion of labeled neurons in laminae A decreased in deprived cats with respect to control, while it increased in the magnocellular lamina C and parvocellular lamina C1. No changes were found in parvocellular lamina C2 and the density decreased in parvocellular lamina C3 (Figs. 9A, B). The distribution of labeled neurons in the MIN in EVD cats was not significantly

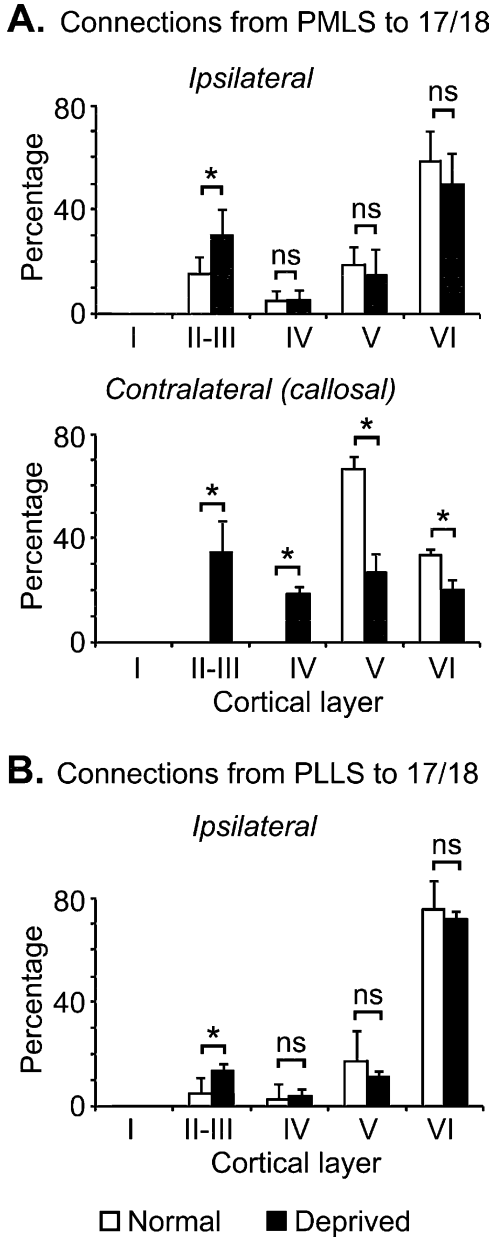

Fig. 8. Radial distribution of labeled neurons in PMLS and PLLS. Percentages of retrogradely labeled neurons per section in control (white bars) and EVD (black bars) cats in different cortical layers of PMLS (A) and PLLS (B). Note the increased number of ipsilaterally labeled neurons in layers II–III in EVD cats with respect to controls, in both PMLS (A) and PLLS (B) areas. In the contralateral hemisphere, callosally projecting neurons from supragranular layers of PMLS were exclusive of EVD cats (A). Vertical lines represent standard deviations. (*): significant differences ($p < 0.05$); ns: nonsignificant differences.

different from the one in control cats, although the density of labeled neurons was lower (Figs. 9A, B). No labeled neurons were found either in the contralateral dLGN or in the ipsilateral and contralateral MGN. No differences either in the distribution or in the density of labeled neurons were found between the control and LVD cats.

Immunolabeling to calretinin, parvalbumin and calbindin D-28 K in areas 17 and 18

Four control, four EVD and one LVD cats were processed for the immunohistochemical study. In control cats, the radial distribution of neurons immunoreactive to calretinin, parvalbumin and calbindin D-28 K and the qualitative characteristics of the immunostaining of these markers in cortical areas 17 and 18 were similar to those previously described (Demeulemeester et al., 1991; Hof et al., 1999; Huxlin and Pasternak, 2001). Density of immunoreactive neurons in areas 17 and 18 of the LVD cat was not significantly different from that in the control cats.

In both control and deprived cats (LVD and EVD), calretinin immunolabeling was observed in nonpyramidal neurons, commonly with features of bipolar neuron such as long, vertically oriented processes (Figs. 10A–D). Labeling of processes and terminal-like puncta was not homogeneous across cortical layers. In particular, in layer IV and upper half of layer V, numerous puncta were present in the neuropil and around unstained cell somata, but no basket formations were found (Figs. 10C, D). In both control and EVD cats, calretinin-immunoreactive neurons were found in all cortical layers with a higher density in layers I–IV (Figs. 10A, B). However, the density of positive neurons in these areas was lower in EVD cats: in area 17 of the EVD cats, there was a 57.8% reduction in positive calretinin neurons with respect to controls and a reduction of 28.1% in area 18 (Fig. 11B).

In all experimental groups, parvalbumin immunolabeling revealed terminal-like puncta and processes in all cortical layers, except layer I (Figs. 10E–H). One of the most conspicuous characteristics was the labeling of numerous terminal-like

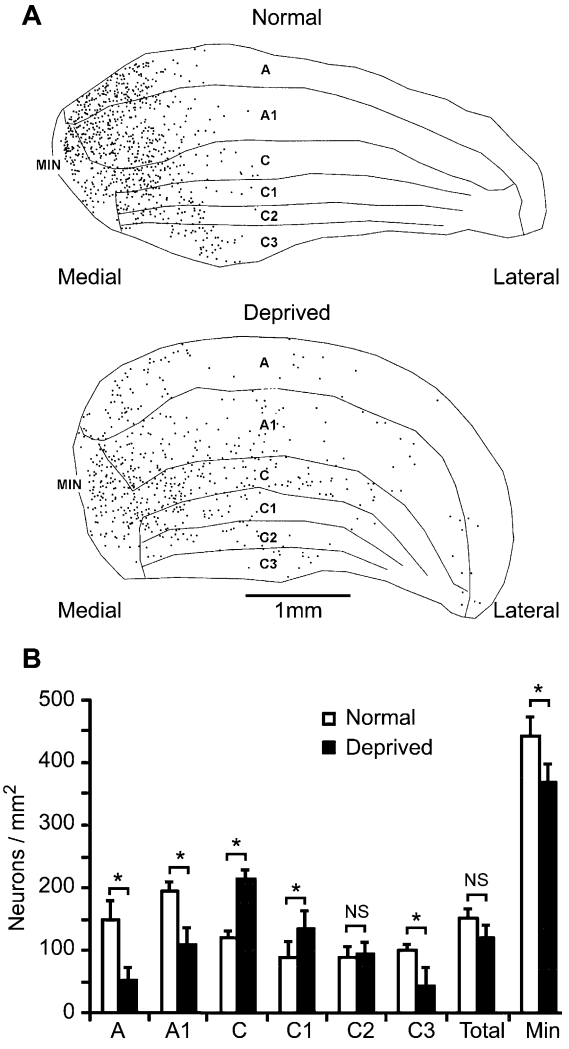

Fig. 9. Distribution of retrogradely labeled neurons in dLGN and MIN in control and EVD cats. (A) In both control and EVD cats, labeled neurons were found in all laminae of the dLGN and MIN. However, in control cats, the density of labeled neurons in the medial half of the dLGN was higher than that in EVD cats, in which labeled neurons had a more widespread distribution. The borders between laminae are indicated. (B) Histograms representing the density of retrogradely labeled neurons in control and EVD cats in different laminae of the dLGN and MIN. Vertical lines represent standard deviations. (*): significant differences ($p<0.05$); ns: nonsignificant differences.

puncta around unstained neuronal somata in layers II–III and especially in layer V, where many large unstained pyramidal neurons were seen surrounded by a very dense plexus of parvalbumin immunoreactive terminal-like puncta (Figs. 10G, H). These perisomatic plexi were similar to the parvalbumin immunoreactive basket formations described in the primate neocortex (i.e. Hendry et al., 1989; Akil and Lewis, 1992). In layers IV and VI, perisomatic terminals were also seen around unlabeled cells but they were fewer: dense basket formations were not seen in these layers. Parvalbumin immunolabeling also marked many positive neuronal somata resembling spiny multipolar interneurons. The size and shape of the labeled neurons were variable, but the majority displayed an ovoid cell body (Figs. 10G, H). In all experimental groups, parvalbumin immunoreactive neurons were found in all cortical layers, except layer I, with a higher density in layer IV (Figs. 10E, F and 11A). As with calretinin immunolabeling, the density of parvalbumin immunoreactive neurons in areas 17 and 18 was lower in EVD cats. In area 17 of deprived cats, a 36.2% reduction was found with respect to controls, and a 22.2% reduction was observed in area 18 (Fig. 11B).

The calbindin D-28 K immunolabeling did not reveal any difference — neither qualitative nor quantitative — between control and both groups of deprived cats (Figs. 10I–L and 11B). In both control and deprived cats, calbindin D-28 K immunoreactivity was observed mainly in cell bodies and dendrites (Fig. 10K–L). Labeling of axonal plexuses and terminal-like buttons was scarce and mostly located in layers II–III, IV and V. In both groups of cats, calbindin D-28K immunoreactive neurons were present in all layers, but the intensity of cell bodies staining varied from light to dark: lightly stained cells were predominant in layers II and III, and cells were more darkly stained in layers IV–VI. The morphology of stained cells varied; many lightly stained cells of layers II–III could be identified as pyramidal neurons, whereas the vast majority of darkly stained cells of layers II–VI were nonpyramidal cells with rounded or fusiform somata (Fig. 11K, L).

Discussion

This study is the first to our knowledge to describe synaptic responses to sound stimuli in areas 17 and border 17/18 of the cat visual cortex. Suprathreshold

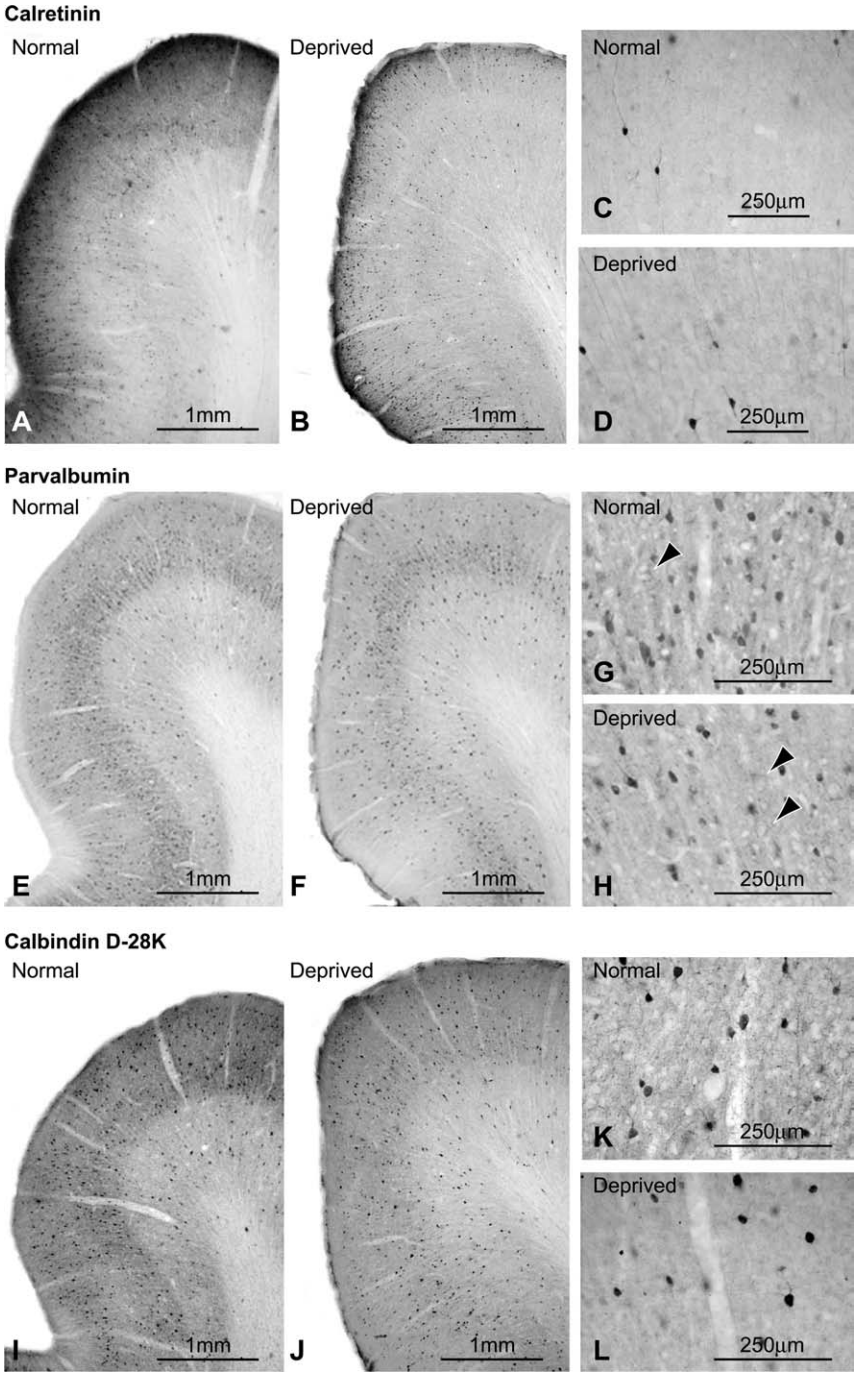

Fig. 10. Photomicrographs through the area 17 stained immunocytochemically for calretinin, parvalbumin and calbindin D-28K in control and EVD cats. (A–D) Calretinin immunostaining in control (A and C) and EVD (B and D) cats. Note that the shape of immunostained neurons in EVD (C) cats is similar to controls (D). (E–H) Parvalbumin immunostaining in control (E and G) and EVD (F and H) cats. G and H are higher-magnification photomicrographs showing immunoreactive neurons and perisomatic puncta (arrowheads) in layer V. The shape of immunoreactive neurons, processes and puncta were similar in EVD (G) and control (H) cats. (I–L) Calbindin D-28K immunostaining in control (I and K) and EVD (J and L) cats. Several immunoreactive nonpyramidal cells in control (K) and EVD (L) cats are shown. In both groups of cats, the morphology of immunoreactive neurons is similar.

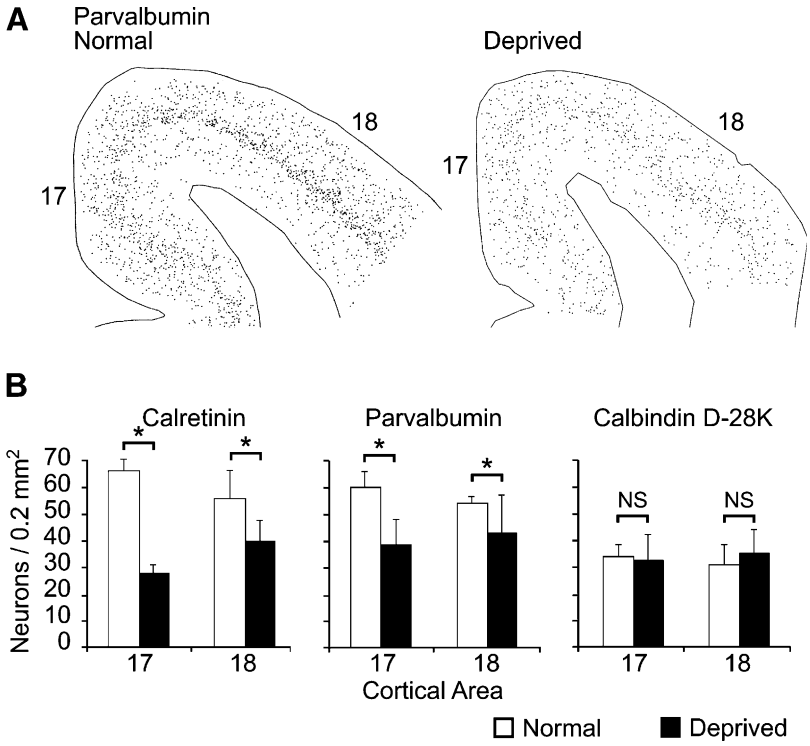

Fig. 11. Distribution of calretinin and parvalbumin-labeled neurons (dots) in areas 17 and 18 of control and EVD cats. (A) In both in control and EVD cats, calretinin immunoreactive neurons were mostly found in cortical supragranular layers, while the density of parvalbumin immunoreactive neurons peaked in layer IV. (B) Frequency histograms representing the density of calretinin, parvalbumin and calbindin D-28K immunoreactive neurons in areas 17 and 18 of both control and EVD cats. Note that in both areas 17 and 18, the density of calretinin and parvalbumin decreased in EVD compared to control cats. The density of calbindin D-28K immunoreactive neurons was similar in both groups. (*): significant differences ($p<0.05$); ns: nonsignificant differences.

responses to sound were recorded as well, with the same time course as the subthreshold ones. Responses to sound in visual cortex were only recorded in EVD cats. Although a similar number of neurons were recorded in EVD ($n = 56$) and LVD ($n = 60$) cats, 14.3% of the neurons responded to sound in the visual cortex of EVD and none in either LVD or control cats. This observation is in agreement with most of the literature, where early blindness is reported to convey larger crossmodal plasticity than late-onset blindness. The importance of early age loss of sight is described in a large number of studies (i.e. Cohen et al., 1999; Gougoux et al., 2004, 2005). When tested, auditory responses did not show obvious frequency tuning. In spite of this poor selectivity, these responses did not seem to be due to an unspecific awakening effect: they were of short latency, tightly time-locked to the stimuli, and were never observed in control or LVD animals examined under the same experimental conditions as the EVD ones.

The synaptic potentials evoked by sound in visual cortex must be at least in part excitatory as they were able to induce spike responses. It is also probable that disynaptic inhibition could be evoked by the auditory stimuli — although we failed to detect it — since one of the recorded cells that responded to sound showed the characteristic firing properties of fast-spiking neurons (Fig. 1B) (Nowak et al., 2003; Descalzo et al., 2005), which are known to be inhibitory (McCormick et al., 1985).

The average amplitude of synaptic potentials evoked by sound was small if compared to the ones evoked with visual stimulation. In another study (Nowak et al., 2005a), synaptic response obtained in response to flashing bars, which is not

the optimal stimulus to activate area 17 neurons, presented a mean amplitude of near 4.5 mV, that is, an amplitude 7.5 times larger than the depolarization produced by the auditory stimuli. A comparable difference is also observed for the spiking response which is about 30 spikes/s with flashing bars (Nowak et al., 2005a), approximately 10 times larger than the response obtained here with auditory stimulation. Nevertheless, although synaptic responses were of small amplitude, they were sufficient to modulate the firing rate.

Onset response latencies in response to auditory stimuli, on the other hand, appear to be surprisingly short. The mean synaptic onset latency to auditory stimulation obtained in the present study is 30 ms, which is actually lower than the mean synaptic onset latency of the response to flashing bars, which was on an average 36 ms in Nowak et al. (unpublished results); see also Creutzfeldt and Ito (1968). Similarly, onset latency for the spiking response in visual cortex appears to be similar in response to auditory stimuli (42 ms) compared to visual stimuli (Best et al., 1986; Eschweiler and Rauschecker, 1993; Nowak et al., 2005b) in normal cats. In addition, it has been shown that, in dark-reared rats, visual responses have significantly longer latencies than in normal rats (Benevento et al., 1992). This suggests that, had we tested visual response latencies in the EVD cats, the difference with those obtained with auditory stimuli could have been even larger.

In the primary auditory area of normal cats, onset latencies to sound for both synaptic and spike responses are much shorter (between 10 and 20 ms on an average) in comparison to response latencies to visual stimuli in primary visual cortex (De Ribaupierre et al., 1972; Phillips and Irvine, 1981; Heil and Irvine, 1996; Mendelson et al., 1997; Ojima and Murakami, 2002). This would explain that, if the responses to sound in primary visual cortex in EVD cats originate in association areas, the latency of these responses could still have the same or even shorter latencies than the ones to visual stimuli. This could also be the case if the origin of the responses would be the inferior colliculus, where latencies of the responses to sound are 5–18 ms (Langner and Schreiner, 1988) and it is one of the possible origins that we have not ruled out anatomically (see below).

In this study we did not obtain auditory responses in area 17 of normal and LVD cats. Similarly, Yaka et al. (1999, 2000) could not evoke sound responses in the visual cortex of control cats. This result is at variance with a number of studies from the 1960s and 1970s that reported auditory, somatosensory and noxious responses through either single unit or evoked potential recordings in areas 17, 18 and 19 of normal cats (Jung et al., 1963; Murata et al., 1965; Buser and Bignall, 1967; Spinelli et al., 1968; Morrell, 1972; Fishman and Michael, 1973). In single-unit recordings, 28–47% of the cells responded to non-visual stimuli. However, it is to be noticed that, in contrast to our study and those by Yaka et al., all these previous studies had in common the use of slightly or unanesthetized cats. It has thus been argued that some of these non-visual responses actually corresponded to unspecific awakening reaction to noxious or loud auditory stimuli. This argument was based on the fact that these responses had long latencies (Jung et al., 1963; Murata et al., 1965; Buser and Bignall, 1967), that they were similar to responses evoked by the brainstem reticular formation (Buser and Bignall, 1967), that they induced increases in blood pressure (Murata et al., 1965) and that they were suppressed by doses of anesthetics that coincided with that required to suppress arousal (Murata et al., 1965; Buser and Bignall, 1967). On the other hand, some of these studies (Spinelli et al., 1968; Morrell, 1972; Fishman and Michael, 1973) reported auditory responses in visual cortex that were sufficiently well tuned, either in the spatial or in the frequency domain, to rule out an unspecific awakening effect. Yet even in these cases, the spike latencies reported for individual examples (60 ms in Spinelli et al., 1968; 130 ms in Fishman and Michael, 1973) appeared to be longer than those reported here (42 ms). This suggests that those responses were induced by a more indirect pathway than the one responsible for the response that is described in the current study, a pathway that, in addition, would be gated by the arousal state of the animal. In light of these different results, it is clear that further refinement in the study

of crossmodal plasticity would benefit from the examination of the consequences of visual deprivation on multisensory responses in the visual cortex of awake animals.

In superior colliculus, visual deprivation since birth leads to an increase in the number of neurons that respond to sound stimuli (Vidyasagar, 1978; Rhoades, 1980; Rauschecker and Harris, 1983). Neurons responding to auditory stimuli are even found in the superficial layers of the superior colliculus (Rhoades, 1980; Rauschecker and Harris, 1983), which in normal animals are exclusively visual. The main input sources to the superficial layers of the superior colliculus are the retina and the visual cortex — mostly area 17 and surrounding areas. It is therefore possible that some of the cells responding to auditory stimuli in the superficial layers of the superior colliculus were actually driven by inputs from the visual cortex.

Finally, our observation on the presence of auditory responses in the visual cortex of cats deprived early of sight is in agreement with most of the literature in humans, where early blindness is reported to convey larger crossmodal plasticity than late-onset blindness (i.e. Cohen et al., 1999; Gougoux et al., 2004, 2005). The functional meaning of the many fMRI experiments that have been performed in the study of crossmodal plasticity depends on the precise sources of the signal that was recorded. In light of this important question, our study unambiguously demonstrates that both the input to (synaptic response) and the output from (spiking responses) areas 17 and 18 can be activated by sound stimulation in the visual cortex of animals deprived of vision at an early age.

Origin of the auditory connections generating responses to sound in primary visual cortex

The retrograde tracing experiments were aimed at identifying which connections could have been modified by the visual deprivation and whether this modification could explain the appearance of auditory responses in areas 17 and 18.

Thalamocortical connections in EVD cats did not appear different from those observed in normal cats: retrogradely labeled cells were found in structures that are devoted to the processing of visual information (LGN), but not in nuclei involved in auditory information processing (e.g. MGN). This does not rule out the possibility that the visual cortex of EVD cats received auditory information through a newly formed pathway between auditory and visual subcortical nuclei. For example, Izraeli et al. reported a projection from the inferior colliculus onto the LGN in hamsters that had been binocularly enucleated after birth (Izraeli et al., 2002). Another example of changes in the connections between visual and auditory subcortical nuclei due to visual deprivation is provided by phylogenetic evolution. In the blind mole rat it has been described that thalamocortical connections originated in the LGN are preserved; however, the LGN receives projections from the inferior colliculus, which may underlie the reported responses to sound in visual cortex in that species (Bronchti et al., 2002). It remains to be established whether derivations of a similar kind would also occur after visual deprivation in cats with an intact visual system.

An alternative pathway is one involving the lateral posterior thalamic (LP) complex. Negyessy et al. (2000) have shown that, in enucleated rats, crossmodal plasticity may be achieved through a cortico-thalamo-cortical pathway. In normal rats, the LP nucleus is reciprocally connected with the visual cortex. However, in enucleated rats, the LP nucleus receives an additional heteromodal projection from the somatosensory cortex. The LP might, in addition, receive inputs from the superficial layers of the superior colliculus, where neurons are found to respond to nonvisual stimuli after early onset visual deprivation (Vidyasagar, 1978; Rhoades, 1980; Rauschecker and Harris, 1983).

Another candidate for explaining the presence of auditory responses in areas 17 and 18 of EVD cats could have been the direct connections linking auditory and visual cortex. It has been shown that, in the newborn kitten, the auditory cortex projects onto areas 17 and 18 (Dehay et al., 1984; Innocenti and Clarke, 1984; Innocenti et al., 1988; Innocenti and Berbel, 1991). However, this connection disappears completely after about 1 month of age, except for very few scattered neurons found in

layers 5 and 6 of auditory cortex (Dehay et al., 1984; Innocenti and Clarke, 1984; Innocenti et al., 1988; Innocenti and Berbel, 1991). It seems reasonable to think that visual deprivation could result in a stabilization of this connection. However, in this study we found that the number of cells labeled in the auditory cortex of EVD cats did not differ from the one found in the adult. This is consistent with the observation that even bilateral enucleation fails to stabilize this transitory connection (Innocenti and Clarke, 1984; Innocenti et al., 1988; Innocenti and Berbel, 1991).

Evoked potentials' studies in normal humans have disclosed, under certain conditions, the occurrence of interactions between auditory and visual stimuli at locations corresponding to the primary visual cortex (Giard and Peronnet, 1999; Shams et al., 2001; Arden et al., 2003). These interactions are highly non-linear, in the sense that auditory stimuli alone do not produce detectable activation but are able to modulate the visually evoked potentials. Modulation of visual responses by auditory inputs might be related to the presence of a direct input, on area V1 of the primate, from the primary auditory cortex, as well as from polymodal areas (Falchier et al., 2002). This projection is weak on the part of area V1 that represents the central visual field, but it is far from being negligible when considering the representation of the peripheral visual field, where it has been shown to be as strong as the projection from the visual areas of the superior temporal sulcus (Falchier et al., 2002). Recent studies also revealed auditory-visual interaction at the single-cell level in area V1 of awake behaving monkeys (Wang et al., 2005). Nevertheless, this direct auditory to visual cortex pathway might be specific to primates: in cat visual cortex no such connection has been demonstrated. As mentioned above, retrograde tracer injection in areas 17, 18 and 19 reveals only a very small number of cells in the auditory areas (Dehay et al., 1984, 1988; Innocenti and Clarke, 1984; Innocenti et al., 1988). In addition, anterograde tracer injection in auditory cortex fails to reveal labeled fibers in the visual cortex of normal adult cats (Dehay et al., 1984, 1988; Innocenti et al., 1988).

We found that the main effect of dark rearing on corticocortical connections appears in area PMLS and PLLS. In these areas, dark rearing induced a remodeling of the laminar distribution of projecting neurons to areas 17 and 18. Thus, the projection from PMLS onto areas 17 and 18 in normal cats originates mostly from neurons in the infragranular layers (70–80%) (Bullier et al., 1984b; Symonds and Rosenquist, 1984; Rosenquist, 1985; Segraves and Innocenti, 1985; Kato et al., 1991; Shipp and Grant, 1991; Einstein, 1996; Batardière et al., 1998; Payne and Lomber, 2003). The connections from PLLS to areas 17 and 18 (a weak projection in normal cats) originate as well almost exclusively from infragranular layers (Symonds and Rosenquist, 1984; Rosenquist, 1985; Segraves and Innocenti, 1985; Payne and Lomber, 2003). After EVD, we have observed a change in the balance of the projections, such that the proportion of connections originated in supragranular layers significantly increases.

Is it possible that these changes in connectivity pattern were responsible for the presence of auditory responses in the visual cortex. PMLS is strongly connected with area AMLS (Symonds and Rosenquist, 1984; Hilgetag and Grant, 2000). AMLS is an area in which neurons appear to respond to both auditory and visual stimuli (Yaka et al., 1999) and where visual deprivation further increases the number of cells responding to auditory stimulation (Yaka et al., 1999). Thus, one possible pathway could involve the increased auditory activity in AMLS together with a remodeling of the projections from PMLS on areas 17 and 18.

Decreased inhibition in visually deprived cats

In this study we have described that EVD cats had a significantly lower number of parvalbumin- and calretinin-positive neurons in areas 17 and 18 than control cats. A general decrease in GAD-positive neurons has also been described in dark reared rats (Benevento et al., 1995; also see Mower and Guo, 2001). Although the number of calbindin-D28K-positive neurons, and probably other subsets of GABAergic neurons remained unchanged, the decrease of parvalbumin- and calretinin-positive neurons found in area 17 is very suggestive of a decreased inhibition in the visual cortex of EVD

cats. Indeed, the decrease of parvalbumine positive (PV)(+) perisomatic synapse formation has been found to decrease with visual deprivation in the mouse (Chattopadhyaya et al., 2004). The functional implications of this decrease are the ones resulting from a decreased inhibition. Different findings reported in the literature are compatible with a decreased inhibition following visual deprivation or dark rearing. Thus, the occipital cortex of humans or animals that have lacked visual input in early ages often presents higher activity than the one in nonvisually deprived subjects. At a cellular level, significantly higher spontaneous activity has been reported in dark reared rats (Benevento et al., 1992; Maffei et al., 2004) and in enucleated hamsters (Izraeli et al., 2002). In the cat, numerous changes in visual responses have been described as a result of dark rearing, such as a lack of sharp inhibitory sidebands and the sometimes exceedingly large size of the receptive fields in areas 17 and 18, which could be due as well to a decreased intracortical inhibition (Singer and Tretter, 1976). A recent characterization of the development of GABAergic transmission in the visual cortex found that inhibition received by layer 2/3 neurons in the rat visual cortex increases during the critical period, but only if there is an exposure to visual stimulation (Morales et al., 2002). Furthermore, only 2 days of visual deprivation profoundly alter the excitatory — inhibitory balance, not only decreasing inhibition but also potentiating excitation (Maffei et al., 2004). In humans, glucose metabolism in striate and prestriate cortical areas was found to be higher in early blind human subjects than in normal-sighted persons (Wanet-Defalque et al., 1988), not only during the realization of tactile and auditory tasks but even at rest. Likewise, studies with functional imaging revealed an increased activity in occipital cortex of the blind that was as well task-independent (Uhl et al., 1993).

The decrease of inhibition that results from visual deprivation has a deep impact on the structure and functionality of the developing cortical circuits, generating an excitation/inhibition disbalance. To what extent one of the functional effects of a decreased inhibition is an increased permissibility for crossmodal plasticity remains to be demonstrated.

Abbreviations

ALLS	anterolateral lateral suprasylvian area
AMLS	anteromedial lateral suprasylvian area
CO	cytochrome oxidase
dLGN	dorsal lateral geniculate nucleus
EVD	early visually deprived
GABA	gamma-aminobutyric acid
GAD	glutamic acid decarboxilase
LVD	late visually deprived
MGN	medial geniculate nucleus
MIN	medial interlaminar nucleus (of dLGN)
PLLS	posterolateral lateral suprasylvian visual area
PMLS	posteromedial lateral suprasylvian visual area
WGA-HRP	wheat germ agglutinin coupled to horseradish peroxidase

Acknowledgments

This work has been sponsored by MCYT (BFI2002-03643) and the European Union IST/FET project PRESENCIA (IST-2001-37927) to MVSV and by Instituto de Salud Carlos III PI03/0576 and Generalitat Valènciana GRUPOS03/053 to PB. LGN was supported by the CNRS and by the Ministry of Foreign Affairs (Egide, ''Picasso'' and CNRS-CSIC joint travel grants). Thanks to Pascal Barone for critical reading of the manuscript. Thank you to M.S. Malmierca and his team for his generous help for the implementation of the auditory stimulation and to J. Merchán for the equipment to do auditory stimulation. We thank the personnel of the animal facilities at the UMH for their effort to keep the visually deprived animals, and in particular the chief veterinarian JA Pérez de Gracia.

References

Akil, M. and Lewis, D.A. (1992) Differential distribution of parvalbumin-immunoreactive pericellular clusters of terminal boutons in developing and adult monkey neocortex. Exp. Neurol., 115: 239–249.

Arden, G.B., Wolf, J.E. and Messiter, C. (2003) Electrical activity in visual cortex associated with combined auditory and visual stimulation in temporal sequences known to be associated with a visual illusion. Vision Res., 43: 2469–2478.

Ashmead, D.H., Wall, R.S., Ebinger, K.A., Eaton, S.B., Snook-Hill, M.M. and Yang, X. (1998) Spatial hearing in children with visual disabilities. Perception, 27: 105–122.

Batardière, A., Barone, P., Dehay, C. and Kennedy, H. (1998) Area-specific laminar distribution of cortical feedback neurons projecting to cat area 17: quantitative analysis in the adult and during ontogeny. J. Comp. Neurol., 396: 493–510.

Benevento, L.A., Bakkum, B.W. and Cohen, R.S. (1995) gamma-Aminobutyric acid and somatostatin immunoreactivity in the visual cortex of normal and dark-reared rats. Brain Res., 689: 172–182.

Benevento, L.A., Bakkum, B.W., Port, J.D. and Cohen, R.S. (1992) The effects of dark-rearing on the electrophysiology of the rat visual cortex. Brain Res., 572: 198–207.

Best, J., Reuss, S. and Dinse, H.R. (1986) Lamina-specific differences of visual latencies following photic stimulation in the cat striate cortex. Brain Res., 385: 356–360.

Bronchti, G., Heil, P., Sadka, R., Hess, A., Scheich, H. and Wollberg, Z. (2002) Auditory activation of ''visual'' cortical areas in the blind mole rat (*Spalax ehrenbergi*). Eur. J. Neurosci., 16: 311–329.

Bullier, J., Kennedy, H. and Salinger, W. (1984a) Bifurcation of subcortical afferents to visual areas 17, 18, and 19 in the cat cortex. J. Comp. Neurol., 228: 309–328.

Bullier, J., Kennedy, H. and Salinger, W. (1984b) Branching and laminar origin of projections between visual cortical areas in the cat. J. Comp. Neurol., 228: 329–341.

Buser, P. and Bignall, K.E. (1967) Nonprimary sensory projections on the cat neocortex. Int. Rev. Neurobiol., 10: 111–165.

Celio, M.R. (1990) Calbindin D-28k and parvalbumin in the rat nervous system. Neuroscience, 35: 375–475.

Celio, M.R., Baier, W., Scharer, L., Gregersen, H.J., de Viragh, P.A. and Norman, A.W. (1990) Monoclonal antibodies directed against the calcium binding protein Calbindin D-28k. Cell Calcium, 11: 599–602.

Chattopadhyaya, B., Di Cristo, G., Higashiyama, H., Knott, G.W., Kuhlman, S.J., Welker, E. and Huang, Z.J. (2004) Experience and activity-dependent maturation of perisomatic GABAergic innervation in primary visual cortex during a postnatal critical period. J. Neurosci., 24: 9598–9611.

Cohen, L.G., Celnik, P., Pascual-Leone, A., Corwell, B., Falz, L., Dambrosia, J., Honda, M., Sadato, N., Gerloff, C., Catala, M.D. and Hallett, M. (1997) Functional relevance of cross-modal plasticity in blind humans. Nature, 389: 180–183.

Cohen, L.G., Weeks, R.A., Sadato, N., Celnik, P., Ishii, K. and Hallett, M. (1999) Period of susceptibility for cross-modal plasticity in the blind. Ann. Neurol., 45: 451–460.

Creutzfeldt, O. and Ito, M. (1968) Functional synaptic organization of primary visual cortex neurones in the cat. Exp. Brain Res., 6: 324–352.

De Ribaupierre, F., Goldstein Jr., M.H. and Yeni-Komshian, G. (1972) Intracellular study of the cat's primary auditory cortex. Brain Res., 48: 185–204.

DeFelipe, J. (1997) Types of neurons, synaptic connections and chemical characteristics of cells immunoreactive for calbindin-D28K, parvalbumin and calretinin in the neocortex. J. Chem. Neuroanat., 14: 1–19.

Dehay, C., Bullier, J. and Kennedy, H. (1984) Transient projections from the fronto-parietal and temporal cortex to areas 17, 18 and 19 in the kitten. Exp. Brain Res., 57: 208–212.

Dehay, C., Kennedy, H. and Bullier, J. (1988) Characterization of transient cortical projections from auditory, somatosensory, and motor cortices to visual areas 17, 18, and 19 in the kitten. J. Comp. Neurol., 272: 68–89.

Demeulemeester, H., Arckens, L., Vandesande, F., Orban, G.A., Heizmann, C.W. and Pochet, R. (1991) Calcium binding proteins and neuropeptides as molecular markers of GABAergic interneurons in the cat visual cortex. Exp. Brain Res., 84: 538–544.

Descalzo, V.F., Nowak, L.G., Brumberg, J.C., McCormick, D.A. and Sanchez-Vives, M.V. (2005) Slow adaptation in fast spiking neurons of visual cortex. J. Neurophysiol., 93: 1111–1118.

Einstein, G. (1996) Reciprocal projections of cat extrastriate cortex: I. Distribution and morphology of neurons projecting from posterior medial lateral suprasylvian sulcus to area 17. J. Comp. Neurol., 376: 518–529.

Eschweiler, G.W. and Rauschecker, J.P. (1993) Temporal integration in visual cortex of cats with surgically induced strabismus. Eur. J. Neurosci., 5: 1501–1519.

Falchier, A., Clavagnier, S., Barone, P. and Kennedy, H. (2002) Anatomical evidence of multimodal integration in primate striate cortex. J. Neurosci., 22: 5749–5759.

Fishman, M.C. and Michael, P. (1973) Integration of auditory information in the cat's visual cortex. Vision Res., 13: 1415–1419.

Fregnac, Y. and Imbert, M. (1984) Development of neuronal selectivity in primary visual cortex of cat. Physiol. Rev., 64: 325–434.

Giard, M.H. and Peronnet, F. (1999) Auditory-visual integration during multimodal object recognition in humans: a behavioral and electrophysiological study. J. Cogn. Neurosci., 11: 473–490.

Gougoux, F., Lepore, F., Lassonde, M., Voss, P., Zatorre, R.J. and Belin, P. (2004) Neuropsychology: pitch discrimination in the early blind. Nature, 430: 309.

Gougoux, F., Zatorre, R.J., Lassonde, M., Voss, P. and Lepore, F. (2005) A functional neuroimaging study of sound localization: visual cortex activity predicts performance in early blind individuals. PLoS Biol., 3: e27.

Heil, P. and Irvine, D.R. (1996) On determinants of first-spike latency in auditory cortex. Neuroreport, 7: 3073–3076.

Hendry, S.H., Jones, E.G., Emson, P.C., Lawson, D.E., Heizmann, C.W. and Streit, P. (1989) Two classes of cortical GABA neurons defined by differential calcium binding protein immunoreactivities. Exp. Brain Res., 76: 467–472.

Hilgetag, C.C. and Grant, S. (2000) Uniformity, specificity and variability of corticocortical connectivity. Philos. Trans. R. Soc. Lond. B Biol. Sci., 355: 7–20.

Hof, P.R., Glezer, II., Conde, F., Flagg, R.A., Rubin, M.B., Nimchinsky, E.A. and Vogt Weisenhorn, D.M. (1999) Cellular distribution of the calcium-binding proteins parvalbumin, calbindin, and calretinin in the neocortex of mammals: phylogenetic and developmental patterns. J. Chem. Neuroanat., 16: 77–116.

Hollander, H. and Vanegas, H. (1977) The projection from the lateral geniculate nucleus onto the visual cortex in the cat. A quantitative study with horseradish-peroxidase. J. Comp. Neurol., 173: 519–536.

Hubel, D.H., Wiesel, T.N. and LeVay, S. (1977) Plasticity of ocular dominance columns in monkey striate cortex. Philos. Trans. R. Soc. Lond. B Biol. Sci., 278: 377–409.

Huxlin, K.R. and Pasternak, T. (2001) Long-term neurochemical changes after visual cortical lesions in the adult cat. J. Comp. Neurol., 429: 221–241.

Hyvarinen, J., Carlson, S. and Hyvarinen, L. (1981) Early visual deprivation alters modality of neuronal responses in area 19 of monkey cortex. Neurosci. Lett., 26: 239–243.

Innocenti, G.M. and Berbel, P. (1991) Analysis of an experimental cortical network: II. Connections of visual areas 17 and 18 after neonatal injections of ibotenic acid. J. Neural. Transplant., 2: 29–54.

Innocenti, G.M., Berbel, P. and Clarke, S. (1988) Development of projections from auditory to visual areas in the cat. J. Comp. Neurol., 272: 242–259.

Innocenti, G.M. and Clarke, S. (1984) Bilateral transitory projection to visual areas from auditory cortex in kittens. Brain Res., 316: 143–148.

Izraeli, R., Koay, G., Lamish, M., Heicklen-Klein, A.J., Heffner, H.E., Heffner, R.S. and Wollberg, Z. (2002) Cross-modal neuroplasticity in neonatally enucleated hamsters: structure, electrophysiology and behaviour. Eur. J. Neurosci., 15: 693–712.

Jung, B., Kornhuber, H. and Da Fonseca, J. (1963) Multisensory convergence on cortical neurons. Neuronal effects of visual, acoustic and vestibular stimuli in the superior convolutions of the cat's cortex. In: Moruzzi, G., Fessard, A. and Jasper, H.H. (Eds.), Brain Mechanisms, Progress in Brain Research, Vol. 1. Elsevier, Amsterdam, pp. 240–270.

Kato, N., Ferrer, J.M. and Price, D.J. (1991) Regressive changes among corticocortical neurons projecting from the lateral suprasylvian cortex to area 18 of the kitten's visual cortex. Neuroscience, 43: 291–306.

Keller, G. and Innocenti, G.M. (1981) Callosal connections of suprasylvian visual areas in the cat. Neuroscience, 6: 703–712.

Korte, M. and Rauschecker, J.P. (1993) Auditory spatial tuning of cortical neurons is sharpened in cats with early blindness. J. Neurophysiol., 70: 1717–1721.

Kujala, T., Alho, K., Huotilainen, M., Ilmoniemi, R.J., Lehtokoski, A., Leinonen, A., Rinne, T., Salonen, O., Sinkkonen, J., Standertskjold-Nordenstam, C.G. and Naatanen, R. (1997) Electrophysiological evidence for cross-modal plasticity in humans with early and late-onset blindness. Psychophysiology, 34: 213–216.

Kujala, T., Huotilainen, M., Sinkkonen, J., Ahonen, A.I., Alho, K., Hamalainen, M.S., Ilmoniemi, R.J., Kajola, M., Knuutila, J.E., Lavikainen, J., et al. (1995) Visual cortex activation in blind humans during sound discrimination. Neurosci. Lett., 183: 143–146.

Langner, G. and Schreiner, C.E. (1988) Periodicity coding in the inferior colliculus of the cat. I. Neuronal mechanisms. J. Neurophysiol., 60: 1799–1822.

Lessard, N., Pare, M., Lepore, F. and Lassonde, M. (1998) Early blind human subjects localize sound sources better than sighted subjects. Nature, 395: 278–280.

Maciewicz, R.J. (1975) Thalamic afferents to areas 17, 18 and 19 of cat cortex traced with horseradish peroxidase. Brain Res., 84: 308–312.

Maffei, A., Nelson, S.B. and Turrigiano, G.G. (2004) Selective reconsfiguration of layer 4 visual cortical circuitry by visual deprivation. Nat. Neurosci., 7(12): 1353–1359.

McCormick, D.A., Connors, B.W., Lighthall, J.W. and Prince, D.A. (1985) Comparative electrophysiology of pyramidal and sparsely spiny stellate neurons of the neocortex. J. Neurophysiol., 54: 782–806.

Mendelson, J.R., Schreiner, C.E. and Sutter, M.L. (1997) Functional topography of cat primary auditory cortex: response latencies. J. Comp. Physiol. [A], 181: 615–633.

Merabet, L., Thut, G., Murray, B., Andrews, J., Hsiao, S. and Pascual-Leone, A. (2004) Feeling by sight or seeing by touch? Neuron, 42: 173–179.

Mesulam, M.M. (1978) Tetramethyl benzidine for horseradish peroxidase neurohistochemistry: a non-carcinogenic blue reaction product with superior sensitivity for visualizing neural afferents and efferents. J. Histochem. Cytochem., 26: 106–117.

Morales, B., Choi, S.Y. and Kirkwood, A. (2002) Dark rearing alters the development of GABAergic transmission in visual cortex. J. Neurosci., 22: 8084–8090.

Morrell, F. (1972) Visual system's view of acoustic space. Nature, 238: 44–46.

Mower, G.D. and Guo, Y. (2001) Comparison of the expression of two forms of glutamic acid decarboxylase (GAD67 and GAD65) in the visual cortex of normal and dark-reared cats. Brain Res. Dev. Brain Res., 126: 65–74.

Murata, K., Cramer, H. and Bach-y-Rita, P. (1965) Neuronal convergence of noxious, acoustic, and visual stimuli in the visual cortex of the cat. J. Neurophysiol., 28: 1223–1239.

Negyessy, L., Gal, V., Farkas, T. and Toldi, J. (2000) Cross-modal plasticity of the corticothalamic circuits in rats enucleated on the first postnatal day. Eur. J. Neurosci., 12: 1654–1668.

Nowak, L.G., Azouz, R., Sanchez-Vives, M.V., Gray, C.M. and McCormick, D.A. (2003) Electrophysiological classes of cat primary visual cortical neurons *in vivo* as revealed by quantitative analyses. J. Neurophysiol., 89: 1541–1566.

Nowak, L.G., Sanchez-Vives, M.V. and McCormick, D.A. (2005a) Role of synaptic and intrinsic membrane properties

in short term receptive field dynamics in cat area 17. J. Neurosci., 25: 1866–1880.
Ojima, H. and Murakami, K. (2002) Intracellular characterization of suppressive responses in supragranular pyramidal neurons of cat primary auditory cortex *in vivo*. Cereb. Cortex, 12: 1079–1091.
Payne, B.R. and Lomber, S.G. (2003) Quantitative analyses of principal and secondary compound parieto-occipital feedback pathways in cat. Exp. Brain Res., 152: 420–433.
Phillips, D.P. and Irvine, D.R. (1981) Responses of single neurons in physiologically defined primary auditory cortex (AI) of the cat: frequency tuning and responses to intensity. J. Neurophysiol., 45: 48–58.
Rauschecker, J.P. and Harris, L.R. (1983) Auditory compensation of the effects of visual deprivation in the cat's superior colliculus. Exp. Brain Res., 50: 69–83.
Rauschecker, J.P. and Korte, M. (1993) Auditory compensation for early blindness in cat cerebral cortex. J. Neurosci., 13: 4538–4548.
Rees, A., Sarbaz, A., Malmierca, M.S. and Le Beau, F.E. (1997) Regularity of firing of neurons in the inferior colliculus. J. Neurophysiol., 77: 2945–2965.
Rhoades, R.W. (1980) Effects of neonatal enucleation on the functional organization of the superior colliculus in the golden hamster. J. Physiol., 301: 383–399.
Roder, B., Rosler, F. and Spence, C. (2004) Early vision impairs tactile perception in the blind. Curr. Biol., 14: 121–124.
Roder, B., Teder-Salejarvi, W., Sterr, A., Rosler, F., Hillyard, S.A. and Neville, H.J. (1999) Improved auditory spatial tuning in blind humans. Nature, 400: 162–166.
Rosenquist, A.C. (1985) Connections of visual cortical areas in the cat. In: Peters, A. and Jones, E.G. (Eds.), Cerebral Cortex. Plenum, New York, pp. 81–117.
Sadato, N., Pascual-Leone, A., Grafman, J., Ibanez, V., Deiber, M.P., Dold, G. and Hallett, M. (1996) Activation of the primary visual cortex by Braille reading in blind subjects. Nature, 380: 526–528.
Sanchez-Vives, M.V. and McCormick, D.A. (2000) Cellular and network mechanisms of rhythmic recurrent activity in neocortex. Nat. Neurosci., 3: 1027–1034.
Sanchez-Vives, M.V., Nowak, L.G. and McCormick, D.A. (2000a) Membrane mechanisms underlying contrast adaptation in cat area 17 *in vivo*. J. Neurosci., 20: 4267–4285.
Sanchez-Vives, M.V., Nowak, L.G. and McCormick, D.A. (2000b) Membrane mechanisms underlying contrast adaptation in cat area 17 *in vivo*. J. Neurosci., 20: 4267–4285.
Segraves, M.A. and Innocenti, G.M. (1985) Comparison of the distributions of ipsilaterally and contralaterally projecting corticocortical neurons in cat visual cortex using two fluorescent tracers. J. Neurosci., 5: 2107–2118.
Segraves, M.A. and Rosenquist, A.C. (1982) The distribution of the cells of origin of callosal projections in cat visual cortex. J. Neurosci., 2: 1079–1089.
Shams, L., Kamitani, Y., Thompson, S. and Shimojo, S. (2001) Sound alters visual evoked potentials in humans. Neuroreport, 12: 3849–3852.
Sherman, S.M. and Spear, P.D. (1982) Organization of visual pathways in normal and visually deprived cats. Physiol. Rev., 62: 738–855.
Shipp, S. and Grant, S. (1991) Organization of reciprocal connections between area 17 and the lateral suprasylvian area of cat visual cortex. Vis. Neurosci., 6: 339–355.
Singer, W. and Tretter, F. (1976) Unusually large receptive fields in cats with restricted visual experience. Exp. Brain Res., 26: 171–184.
Spear, P.D., Tong, L. and Langsetmo, A. (1978) Striate cortex neurons of binocularly deprived kittens respond to visual stimuli through the closed eyelids. Brain Res., 155: 141–146.
Spinelli, D.N., Starr, A. and Barrett, T.W. (1968) Auditory specificity in unit recordings from cat's visual cortex. Exp. Neurol., 22: 75–84.
Steriade, M., Nunez, A. and Amzica, F. (1993) A novel slow (<1 Hz) oscillation of neocortical neurons *in vivo*: depolarizing and hyperpolarizing components. J. Neurosci., 13: 3252–3265.
Symonds, L.L. and Rosenquist, A.C. (1984) Corticocortical connections among visual areas in the cat. J. Comp. Neurol., 229: 1–38.
Toldi, J., Joo, F., Feher, O. and Wolff, J.R. (1988) Modified distribution patterns of responses in rat visual cortex induced by monocular enucleation. Neuroscience, 24: 59–66.
Toldi, J., Rojik, I. and Feher, O. (1994) Neonatal monocular enucleation-induced cross-modal effects observed in the cortex of adult rat. Neuroscience, 62: 105–114.
Uhl, F., Franzen, P., Podreka, I., Steiner, M. and Deecke, L. (1993) Increased regional cerebral blood flow in inferior occipital cortex and cerebellum of early blind humans. Neurosci. Lett., 150: 162–164.
Vidyasagar, T.R. (1978) Possible plasticity in the rat superior colliculus. Nature, 275: 140–141.
Wanet-Defalque, M.C., Veraart, C., De Volder, A., Metz, R., Michel, C., Dooms, G. and Goffinet, A. (1988) High metabolic activity in the visual cortex of early blind human subjects. Brain Res., 446: 369–373.
Wang, Y., Celebrini, S., Trotter, Y. and Barone, P. (2005) Multisensory integration in the behaving monkey: behavioral analysis and electrophysiological evidence in the primary visual cortex. In: *Society for Neuroscience Vol. Program No. 509.2.* SFN Online, Washington, DC.
Wiesel, T.N. and Hubel, D.H. (1965) Comparison of the effects of unilateral and bilateral eye closure on cortical unit responses in kittens. J. Neurophysiol., 28: 1029–1040.
Wong-Riley, M. (1979) Changes in the visual system of monocularly sutured or enucleated cats demonstrable with cytochrome oxidase histochemistry. Brain Res., 171: 11–28.
Yaka, R., Yinon, U., Rosner, M. and Wollberg, Z. (2000) Pathological and experimentally induced blindness induces auditory activity in the cat primary visual cortex. Exp. Brain Res., 131: 144–148.
Yaka, R., Yinon, U. and Wollberg, Z. (1999) Auditory activation of cortical visual areas in cats after early visual deprivation. Eur. J. Neurosci., 11: 1301–1312.